Dentomaxillofacial Radiology (2015) 44, 20140197

birpublications.org/dmfr

CBCT SPECIAL ISSUE: REVIEW ARTICLE

Effective dose of dental CBCT—a meta analysis of published data and additional data for nine CBCT units

[1]J B Ludlow, [2]R Timothy, [3]C Walker, [4]R Hunter, [5]E Benavides, [6]D B Samuelson and [6]M J Scheske

[1]North Carolina Oral Health Institute, Koury Oral Health Sciences, Chapel Hill, NC, USA; [2]Graduate Program in Oral and Maxillofacial Radiology, University of North Carolina, Chapel Hill, NC, USA; [3]Department of Orthodontics, University of Missouri, Columbia, MO, USA; [4]Private Practice of Orthodontics, Houston, TX, USA; [5]University of Michigan School of Dentistry, Ann Arbor, MI, USA; [6]University of North Carolina School of Dentistry, Chapel Hill, NC, USA

Objectives: This article analyses dose measurement and effective dose estimation of dental CBCT examinations. Challenges to accurate calculation of dose are discussed and the use of dose–height product (DHP) as an alternative to dose–area product (DAP) is explored.
Methods: The English literature on effective dose was reviewed. Data from these studies together with additional data for nine CBCT units were analysed. Descriptive statistics, ANOVA and paired analysis are used to characterize the data.
Results: PubMed and EMBASE searches yielded 519 and 743 publications, respectively, which were reduced to 20 following review. Reported adult effective doses for any protocol ranged from 46 to 1073 μSv for large fields of view (FOVs), 9–560 μSv for medium FOVs and 5–652 μSv for small FOVs. Child effective doses from any protocol ranged from 13 to 769 μSv for large or medium FOVs and 7–521 μSv for small FOVs. Effective doses from standard or default exposure protocols were available for 167 adult and 52 child exposures. Mean adult effective doses grouped by FOV size were 212 μSv (large), 177 μSv (medium) and 84 μSv (small). Mean child doses were 175 μSv (combined large and medium) and 103 μSv (small). Large differences were seen between different CBCT units. Additional low-dose and high-definition protocols available for many units extend the range of doses. DHP was found to reduce average absolute error for calculation of dose by 45% in comparison with DAP.
Conclusions: Large exposure ranges make CBCT doses difficult to generalize. Use of DHP as a metric for estimating effective dose warrants further investigation.
Dentomaxillofacial Radiology (2015) **44**, 20140197. doi: 10.1259/dmfr.20140197

Cite this article as: Ludlow JB, Timothy R, Walker C, Hunter R, Benavides E, Samuelson DB, et al. Effective dose of dental CBCT—a meta analysis of published data and additional data for nine CBCT units. *Dentomaxillofac Radiol* 2015; **44**: 20140197.

Keywords: radiation dosage; cone beam computed tomography; humans; phantoms; adult; child

Introduction

The intent of this article is to review the literature on dosimetry of maxillofacial CBCT imaging in dentistry. A discussion of dose outside the context of biological harm has little relevance to patient care; therefore, this report focuses on effective dose, a quantity with direct correlations to biological risk. A number of approaches may be taken to measure dose and calculate effective dose, and some of the advantages and disadvantages of these are explored. Because children are at greater risk from exposure to ionizing radiation, child and adult doses are explored separately. Tables of published effective dose data from all protocols and equivalent dose data from standard CBCT protocols are presented together with previously unreported data for nine CBCT units. Finally, dose–area product (DAP) is contrasted

Correspondence to: Dr John Barrett Ludlow. E-mail: jbl@email.unc.edu

Supported in part by the National Institute of Dental and Craniofacial Research of the National Institutes of Health under award number R21DE022160.
Received 10 June 2014; revised 3 September 2014; accepted 11 September 2014

with dose–height product (DHP) as a potential surrogate for estimating effective dose.

Is dose from maxillofacial radiographic imaging a relevant risk?

Dentistry had an early awareness of the dangers of exposure to ionizing radiation, as pioneers of radiographic imaging such as Edmund Kells suffered carcinoma of the hands resulting from repeated unprotected exposures during imaging of their patients.[1] We were warned about the dangers of radiography to both practitioners and patients by other pioneers such as Rollins.[2] But not all practitioners were convinced that there was a significant risk. In an exchange of letters published in successive February 1901 issues of the weekly predecessor to the *New England Journal of Medicine*, Rollins assertion that "X-light kills" was rebutted by a prominent surgeon, Ernest Codman, stating that "in careful hands, there is no danger from the use of the X-ray *to the patient* and very little to the operator."[3] Although the scientific debate about the level of risk associated with diagnostic imaging continues, there is substantial evidence for a cumulative dose-related response to ionizing radiation in the form of cancer developing years after initial exposure. Some of this evidence comes from the Life Span Study of atomic bomb survivors, a well-documented cohort of 105,427 people exposed to a range of doses.[4] Analysis of these data and data from several other cohorts provides good support for an increased risk of cancer from acute exposures in a range of 10–50 mSv and chronic exposures in a range of 50–100 mSv.[5] This has prompted support by the National Commission on Radiation Protection and Measurements for a linear extrapolation of higher dose-associated cancer risk to lower levels of exposure: "Although other dose–response relationships for the mutagenic and carcinogenic effects of low-level radiation cannot be excluded, no alternate dose–response relationship appears to be more plausible than the linear-non-threshold model on the basis of present scientific knowledge."[6] The Life Span Study data also indicate a significant radiation-associated increase in the risk of cancer occurring in adolescence and young adulthood.[4] Diagnostic imaging contributes to individual and population exposures to ionizing radiation, and it has been suggested that as many as 1.5–2.0% of cancers in the USA may be related to X-ray exposure from CT imaging.[7] Recent studies have confirmed that cancer risk extends to X-ray exposure from diagnostic imaging of the maxillofacial complex. In a Great Britain cohort of approximately 175,000 subjects who were children at the time of CT head scan exposures, cumulative doses of about 50 mGy almost tripled the risk of leukaemia and doses of about 60 mGy almost tripled the risk of brain cancer.[8] Similar findings were seen in an Australian cohort of 10.9 million people aged 0–19 years, where a 24% increase in cancers, including brain cancers and leukaemia, were noted following CT exposure. The incidence was associated with increasing dose and young age at the time of exposure.[9]

CBCT is a form of CT that has been adapted to maxillofacial imaging and has been enthusiastically embraced by dentistry. Since its introduction in the European market in 1996 and in the US market in 2001, 15 different manufacturers have offered 24 CBCT models in the USA and many more worldwide.[10] CBCT use has found its way into many aspects of general and speciality practice, including adolescent orthodontics. Public concern about this particular application has prompted questions from both patients and practitioners about safe use and best practice.[11] While the risk from dentomaxillofacial imaging is small for an individual, when multiplied by the large population of patients who are exposed to diagnostic imaging, radiation risk becomes a significant public health issue.

Measures of exposure to ionizing radiation

Exposure is the simplest measure of radiation dose. A variety of radiation detection devices, including ionization chambers, radiosensitive films, thermo or optical light-stimulated luminescent dosemeters, and metal oxide-semiconductor field-effect transistor devices may be used to measure ionization caused by radiation. Because calcified tissues absorb X-rays more effectively than do soft tissues and because the absorption of X-rays varies substantially with the size and shape of imaged anatomy as well as the distribution of tissues of different densities within that anatomy, exposure in air provides a limited and sometimes misleading indication of the energy imparted to different tissue types and thicknesses.

Measurement of absorbed dose in specific tissues or organs permits estimation of potential harm to a tissue of interest. Because the absorption efficiency of the radiation detection device may be different than the organ of interest, adjustment of measured values to compensate for this is necessary. For example, absorption efficiency of bone may be 2–4 times greater than that of soft tissues for average photon energies in the diagnostic spectrum. Absorbed dose is expressed in the international unit, gray and more commonly for diagnostic imaging in milligray.

Equivalent dose is absorbed dose adjusted for the attenuation characteristics of the radiation that is involved. The attenuating quality of radiation has a significant impact on biological effectiveness for cancer induction and genetic effects. Alpha particle radiation produces numerous ionization events over a short distance in comparison with the energy that is transferred by an X-ray photon over the same distance. The calculation of equivalent dose (H_T) is the product of the absorbed dose (D_T) and a radiation-weighting factor (w_R), which accounts for relative biologic effectiveness of the radiation. While w_R for α particle radiation is 20, the w_R for X-rays is 1. It is convenient, but sometimes confusing, that X-ray absorbed dose and equivalent dose are the same value. Equivalent dose is expressed in international units, sievert and again, for diagnostic imaging, more commonly in millisievert.

Although in some instances it is useful to consider the biological response to an equivalent dose for a particular tissue of interest, it is often desirable to evaluate a variety of exposures of different types and different body areas for a collective outcome such as cancer. The International Commission on Radiological Protection (ICRP) has recommended a calculation called effective dose as the preferred method for comparing risks from different exposures to ionizing radiation. Effective dose is a calculation that considers the most radiosensitive tissues and organs of the body and provides a fractional weighting reflecting the degree of sensitivity for each of those organs. Effective dose is reported in sieverts and for diagnostic imaging is more commonly expressed in millisieverts or microsieverts. Effective dose is calculated using the equation: $E = \sum w_T \times H_T$, where E is the summation of the products of the tissue weighting factor (w_T) and the absorbed dose within that tissue H_T.[12] Because estimation of the risk of the stochastic effects of genetic mutation and cancer formation has evolved with additional data reported from observations of a variety of exposed populations, the ICRP has changed the calculation of effective dose several times. The most recent change was in 2007[13] and is noteworthy because weights of several tissues located in and around the maxillofacial region were changed, and several other tissues within this region were added to the calculation.[14] Changes in tissue weights have resulted in a 10% increase in weight of tissues located in the maxillofacial area and a 28% increase in weight after adjusting for the distribution of tissues. Newly added tissues for effective dose calculation that are entirely within the maxillofacial area include oral mucosa, salivary glands and the extrathoracic airways.

Approaches to measuring dose—do "all roads lead to Rome"?

The process of measuring equivalent dose and calculating effective dose requires a real or virtual device known as a phantom. There are numerous design variations described in the literature or commercially available that include differences in phantom size, material composition and number of dosemeter locations. While all phantoms simulate human morphology and radiation attenuation characteristics to a varying extent, the gold standard method of obtaining dosimetry for calculating effective dose utilizes an anthropomorphic phantom. Alternate techniques for calculating dose that do not use anthropomorphic phantoms include CT dose index volume (CTDIvol), dose linear product, air kerma-area product and DAP. In a previous study comparing an anthropomorphic phantom and a standard acrylic cylinder with a single ion chamber used to calculate (CTDIvol), we demonstrated that the standard acrylic cylinder underestimates effective dose by 38–62%.[15] This underestimation is in part owing to the failure to account for scatter dose to tissues outside of the scan region. Kerma-area product is another method that has recently been used to calculate dose.[16] Values reported in the referenced study underestimate effective dose by 90–300% when compared with effective dose calculated from anthropomorphic phantom data.[17] DAP has also been suggested as a simple approach for calculating dose. However, our experiments with the SCANORA® 3D (Soredex, Helsinki, Finland) unit revealed an approximately three-fold change in effective dose between various locations of the small field of view (FOV) with no change in DAP.[18] By contrast, anthropomorphic phantoms made from materials that have similar X-ray attenuation characteristics as human tissue and have multiple dosemeters allow for accurate measurement of absorbed dose. In a recent study, we confirmed that an anthropomorphic phantom using bone equivalent material in place of a human skeleton could provide reliable measures of effective dose.[19] Virtual phantoms and Monte Carlo simulation of exposure have been used in assessment of organ dose and effective dose for a number of studies. Dose correspondence with anthropomorphic phantom studies is dependent on the virtual phantom that is used as well as imaging geometry and technical parameters. In one study comparing four different phantoms developed from CT data, a 70% difference in effective dose was noted for a large FOV scan depending phantom choice.[20] When a cephalometric analysis was performed on ICRP adult male and female phantoms, a 17° downward rotation difference of the Frankfort plane was seen in the female. This downward rotation of the chin effectively moves the thyroid closer to the radiation field and results in an average of a 3.7-fold increase in female thyroid dose for four large FOVs that were evaluated in one study.[21] Similar increases are seen in oesophageal dose in this phantom. Although the ICRP phantoms were developed for general dosimetric applications, the inability to adjust phantom posture to establish a Frankfort horizontal plane or any orientation other than the original orientation used to acquire axial CT slices limits the accuracy of these phantoms in simulations of dental CBCT diagnostic protocols. Although virtual phantoms with Monte Carlo simulation hold a great deal of promise, further attention must be given to virtual phantom development consistent with positioning for standard dental diagnostic protocols before this becomes a reliable replacement for anthropomorphic phantoms.

Even anthropomorphic phantom systems are subject to variations in dosimetry from a variety of sources. Intended differences in subject size and organ location are seen when comparing child and adult phantoms. Child phantom effective doses are approximately 36% greater than adult phantom doses for the same imaging protocol.[22] This difference is largely related to the proximity of the thyroid gland to the lower border of the mandible. Because of reduced distance between the thyroid and the mandible in a child, direct exposure of the thyroid is more likely and the intensity of scatter radiation from jaw structures to the thyroid is greater.[22]

Use and abuse of effective dose

Effective dose was developed to provide a measure of stochastic risks from exposures to low doses of ionizing radiation. While developed for use in radiation protection, it should not be applied to estimations of individual patient risks. There are several reasons for this. Foremost, effective dose represents risk to a reference subject who is an average of characteristics, including age, gender and genetic radiation sensitivity. Another reason is that effective dose estimation is subject to numerous sources of uncertainty.[23] Among these is the need to extrapolate stochastic outcomes associated with higher doses to the low doses associated with dental diagnostic imaging. X-ray beam shape and imaging geometry for organs partially in or just outside the beam is also estimated to account for as much as ±40% variation. Despite these limitations, effective dose is a useful metric for comparing alternative imaging modalities or examination protocols in terms of relative risk. Employing the same methods of dose measurement for different examinations, units or protocols, we can evaluate which produces a greater or lower risk. The caveat that this risk may be greater or less depending on individual patient characteristics makes the comparison no less valid.

Biological parameters that influence dose

A number of physical and biological parameters influence individual dose and risk. Age has a significant impact on both. Children are physically smaller, which places peripherally located brain and thyroid tissues closer to the dental area that is being imaged. Even if not directly exposed, these organs will receive increased scatter radiation with increased proximity to the location of the scanned volume. But children are not simply small adults. They are also at increased risk from any exposure to ionizing radiation owing to cellular growth and organ development, which increases radiosensitivity of tissues. In conjunction with a longer life expectancy in which cancer can develop, children may be two times or more sensitive to radiation carcinogenesis than are mature adults.[24,25] Physical differences associated with gender are also associated with differences in risk. Females are at significant risk for breast cancer, while males are not. Females are at risk for ovarian cancer, while males are at risk for prostate cancer. Because these organs are distant from the maxillofacial area, gender differences do not impact dose and risk estimation for maxillofacial imaging.

Technical parameters that influence dose

Receptor technology and field of view: Multiple technical parameters influence patient dose. Two types of receptor technologies are used to acquire image data. Image intensifiers utilize a round receptor and produce a spherical FOV. Square or rectangular flat panel detectors are incorporated in many CBCT units, and these produce a cylindrical FOV. In general, the cylindrical field is more efficient at capturing the anatomy of the maxillofacial complex when the top of the field includes the temporomandibular joint areas. A cylindrical volume diameter, which captures both temporomandibular joint and chin anatomy will require a spherical volume diameter that is approximately 25% larger to cover the same anatomy.

mAs: X-ray tube current (mA) and exposure time (s) are directly proportional to dose when other factors remain constant. The product of mA and s (mAs) is also directly proportional. For instance, doubling mAs doubles dose. It should be mentioned that exposure time may not be the same value as scanning time. Some CBCT units produce continuous output of radiation during scanning. For these units, scan time is equal to exposure time. However, most detectors are unable to record X-ray exposure during the period when the image detector integrates the X-ray energy absorbed in individual receptor pixels and transfers this signal to the computer. Continued X-ray exposure during signal integration contributes to patient dose but adds nothing to image formation. To eliminate this unnecessary patient exposure, many CBCT units utilize a pulsed X-ray source, where X-ray emission is intermittently turned off during the image acquisition process.

kVp and beam filtration: X-ray beam quality has long been noted as a factor associated with patient dose from diagnostic imaging. Increasing filtration of the X-ray beam reduces patient exposure to lower energy X-ray photons that are more likely to contribute to patient dose without contributing to image formation.[26] While higher beam energies (kV) are associated with loss of contrast in film-based imaging, digital imaging affords the possibility of post-acquisition contrast enhancement. Use of 0.4 mm of additional copper filtration in conjunction with increased kVp was demonstrated to reduce patient dose by an average of 43% with one unit.[10] In a study of a different manufacturer's unit, the effective dose for a standard exposure with an 8×8-cm FOV was reduced 57% using 0.5 mm of additional copper filtration when compared with the dose produced by an earlier version of the unit.[15,19]

Resolution: In order to maintain adequate signal-to-noise level, exposure must be increased as the voxel size is reduced to create higher resolution images. This can take place as an increase in mA or an increase in the number of basis images that are acquired. With some CBCT units, this choice is under operator control, but, at other times, the unit dictates which exposure factors may be used with different resolutions. Automatic doubling of dose when switching from standard to high resolution has been reported for one unit.[22]

Methods and materials

Systematic review of literature on CBCT and effective dose

A systematic review of the literature concerning CBCT dosimetry in the maxillofacial region was performed.

A PubMed (MEDLINE) database (National Library of Medicine, NCBI) search was performed on 11 November 2013 and updated on 26 May 2014. An EMBASE search was also performed on 26 May 2014 by a senior librarian at the University of North Carolina Health Science Library, Chapel Hill, NC. The strategy to search for publications in English language indexed in the MEDLINE database was as follows: {"Cone-Beam Computed Tomography" [(Mesh)] OR CBCT (tw) OR CBVT (tw) OR Cone beam computed tomography (tw) OR Cone beam volumetric tomography (tw)} AND ["Radiation Monitoring" (Mesh) OR "Radiation dosage" (Mesh) OR absorbed dos* (tw) OR equivalent dos* (tw) OR effective dos* (tw) OR dosimetry (tw)]. The strategy to search for publications in English language indexed in the EMBASE database was as follows: ("cone beam computed tomography"/exp OR "cone beam computed tomography scanner"/exp OR CBCT:ti,ab OR CBVT:ti,ab OR "Cone beam computed tomography":ti,ab OR "Cone beam volumetric tomography":ti,ab) AND ("radiation monitoring"/exp OR "radiation dose"/exp OR "dosimetry"/exp OR "absorbed dose":ti,ab OR "absorbed doses":ti,ab OR "absorbed dosage":ti,ab OR "absorbed dosages":ti,ab OR "equivalent dose":ti,ab OR "equivalent doses":ti,ab OR "equivalent dosage":ti,ab OR "equivalent dosages":ti,ab OR "effective dose":ti,ab OR "effective doses":ti,ab OR "effective dosage":ti,ab OR "effective dosages":ti,ab). The PubMed search yielded 519 articles and the EMBASE search yielded 743 articles. Inclusion criteria for this review were all articles published in English in the scientific literature related to CBCT dosimetry in the maxillofacial region. Only articles utilizing tissue weights from the 2007 ICRP recommendations for calculating effective dose were included. The articles had to include pertinent information regarding the scanner used, FOV size and location, exposure technique, phantom type and dosemeter used. Articles not meeting the inclusion criteria were excluded after downloading the references in EndNote® (Thompson Reuters, Rochester, NY) and reviewing the abstracts. 65 articles were initially included and the PDF of the articles were downloaded in EndNote and reviewed in more detail. 43 more articles were excluded leaving 22 articles. Data from these studies were placed in a spreadsheet for analysis. Data identified as outliers led to the identification of methodological errors resulting in the removal of two studies and reassessment of the data. Data from 20 studies and additional unpublished data otherwise meeting the inclusion criteria were ultimately tabulated and presented in this article. Reasons for exclusion of the 43 manuscripts are catalogued in Table 1.

Table 1 Reasons for exclusion of 45 of 65 citations resulting from literature search

Reason for exclusion	*Number*
Dosimetry based on 1990 International Commission on Radiological Protection calculation of effective dose rather than 2007 recommendations	6
Image-guided radiation therapy device or other non-dental unit	10
Incomplete dosimetry—multiple organs in the head and neck area have been omitted including remainder tissues	6
Not a dosimetry article, a review article, letter or other secondary source	7
Technique article that does not provide information about specific or identifiable units	3
Effective dose not reported	9
Animal study or anatomy other than maxillofacial area	2
Foreign language with English abstract	1
Other—reported results violate dose/mAs linearity by ×3 indicating an unrecognized calculation error	1

Additional dosimetry

Previously unreported data are included for nine additional CBCT units: 3D Accuitomo (J Morita, Osaka, Japan), CS 9000 (Carestream Dental, Atlanta, GA), CS 9300 (Carestream Dental), Orthophos XG 3D (Sirona Dental Systems, Bensheim, Germany), Galileos Comfort Plus (Sirona Dental Systems), ProMax Mid (Planmeca Oy, Helsinki, Finland), NewTom VGi (Cefla Dental Group, Imola, Italy) and OP 300 Maxio (Instrumentarium, Helsinki, Finland). Scanning protocols for these units are found in Table 2.

Following previously published protocols that utilize 24 dosemeters placed in and on anthropomorphic phantoms, dosimetry was acquired for standard imaging protocols and additional protocols when available. Head and neck phantoms replicating the radiation attenuation characteristics of human tissues and anatomy were used.[15,22] The child phantom (Atom Model 706 HN; CIRS Inc., Norfolk, VA) simulated characteristics of a 10-year-old child. An adult phantom simulated an average adult male (Atom Max Model 711 HN; CIRS Inc.).

Optically stimulated luminescent dosemeters (nanoDot™, Landauer, Inc., Glenwood, IL) were cleared of ambient charge prior to use, using a minimum of 12 h of exposure to light from a florescent tube, dental radiographic film view box. Dosemeters were read to record residual baseline energy level using a portable reader (MicroStar; Landauer, Inc.). The reader was calibrated before use using a set of 80-kVp reference dosemeters supplied by the manufacturer. After adjusting for individual dosemeter energy sensitivity, photon counts were converted to dose and automatically recorded in a database by the reader. After placement in a phantom and exposure to the CBCT scan, dosemeters were read three times with the reader. The modal value of the three readings was selected as the dose of the dosemeter. Doses were exported from the database as an Excel® (Microsoft, Redmond, WA) spreadsheet and adjusted for response to the estimated mean energy of the X-ray beam using a third-order polynomial calibration curve derived from side-by-side comparison of recorded doses from an ion chamber and optical stimulated luminescent dosemeters over a range of 80–120 kVp using an adjustable kVp source. Beam energy adjustments ranged from 0.97 for an 84-kVp source (mean kV = 56)

Table 2 Units and protocols used to produce unreported dosimetry included in this manuscript

CBCT unit	*Manufacturer*	*Phantom type*	*Protocol*	*Field of view*
3D Accuitomo	J Morita (Osaka, Japan)	Atom child, adult	Standard, high fidelity, high resolution, high speed/360°, 180° scans/child, average adult, large adult	Large, medium, small
CS 9000	Carestream Dental (Atlanta, GA)	Rando adult	Standard	Small
CS 9300	Carestream Dental	Atom child, adult	Standard	Medium, small
Orthophos XG 3D	Sirona Dental Systems (Bensheim, Germany)	Atom child, adult	Standard, high definition, endo/child, teen, small adult, average adult, large adult	Small
Galileos® Comfort Plus	Sirona Dental Systems	Atom child, adult	Standard, high definition/child, teen, small adult, average adult, large adult	Medium, small
ProMax® Mid	Planmeca Oy (Helsinki, Finland)	Atom child, adult	Normal, low dose, high definition/ child, adolescent, small adult, average adult, large adult	Medium
NewTom VGi	Cefla Dental Group (Imola, Italy)	Rando adult	Standard, high resolution	Medium, small
NewTom 3G	Cefla Dental Group	Atom child	Standard	Large, medium
OP 300 Maxio	Instrumentarium (Helsinki, Finland)	Atom child, adult	Standard, low dose, high definition, endo/child, small adult, regular adult, large adult	Medium, small

to 0.78 for a 120-kVp source (mean kV = 80). 2–20 exposures were utilized for each dosemeter run to provide a more reliable measure of radiation in the dosemeters. Smaller FOVs require more exposure repetition because more dosemeters are outside the field of direct exposure and absorb only small quantities of scatter radiation. For every scan, a scout view was also acquired. Dosemeter values were divided by the number of scans to determine the "exposure per examination" for each dosemeter.

Absorbed dose for a tissue or organ used in the estimation of effective dose was calculated by averaging doses for dosemeters located within that tissue and are reported in micrograys (μGy).[22] In instances where tissues were not fully contained within the head and neck area, an estimation of the proportion of this tissue within this area was used to calculate organ absorbed dose. For skin surface, lymph nodes and muscle, an estimate of 5% was used. For the oesophageal tract, an estimate of 10% was used. Calculations for bone surface and bone marrow were adjusted for calvarial, jaw or spine location as well as phantom type (child, adult) using estimations of Underhill et al[27] for bone distribution and Christy[28] for marrow distribution. For bone, a correction factor based on experimentally determined mass energy attenuation coefficients for bone and muscle irradiated with monoenergetic photons was applied. Effective beam energy estimated to be two-thirds of the peak beam energy of the CBCT unit was used to determine bone/muscle attenuation ratios. A linear fit ($R^2 = 0.996$) of ratios from 40 to 80 kV from published data[29] was used to calculate bone/muscle ratio for the CBCT unit kVp setting. Calculated values provided bone/muscle attenuation ratios from 3.46 at 54.0 kV (84 kV peak) to 1.97 at 80 kV (120 kV peak) for the units and protocols investigated in this study. The products of absorbed dose and the percentage of a tissue or organ irradiated in the CBCT examination were used to calculate equivalent dose in microsieverts (μSv). Effective dose (E), expressed in μSv, was calculated using ICRP 2007 tissue weighting factors.[13]

Data analysis

Effective doses for various exposure parameters and protocols are reported in a tabular format together with equivalent doses from standard or default CBCT imaging if these were included in the publication. Means and variance for data grouped by child or adult phantom and small, medium and large FOVs are reported in summary tables. For this manuscript, small FOVs are defined as any field with a height ≤10 cm. Medium FOVs include a range of volume heights from 10 to 15 cm. Large FOVs have volume heights >15 cm. ANOVA is used to distinguish differences in equivalent doses or effective doses owing to the variables of phantom and FOV. An additional ANOVA examines the effect of maxillary or mandibular position on effective dose for small FOVs. An α level of 0.05 was selected for statistical significance.

The product of salivary gland dose and the dimensions of FOV ($H \times W$) are used as a surrogate for DAP to calculate conversion coefficients for effective dose estimation. Similarly, the product of salivary gland dose and volume height alone (DHP) is calculated to investigate the possible use of this metric for calculating effective dose conversion coefficients. This is analogous to the product of CTDI and scan length (dose–length product) as a dose metric in CT imaging. The absolute error between the estimated effective dose derived from DAP and the phantom dose measurement was compared with absolute error between DHP-derived dose and phantom measurement in a matched pairs analysis.

Results

Table 3 displays exposure parameters and doses for an adult phantom and large FOVs. Reported effective

Table 3 Adult phantom equivalent and effective doses for standard or default exposures for large field of view (FOV) CBCT units (>15 cm height)

Unit name	*Manufacturer*	*FOV size* H × W *(cm)*	*kVp*	*mAs*	*Effective dose (μSv)*	*Bone marrow (μSv)*	*Bone surface (μSv)*	*Skin (μSv)*	*Oesophagus (μSv)*	*Brain (μSv)*	*Thyroid (μSv)*	*Salivary glands (μSv)*	*Remainder (μSv)*	*Study*
ProMax Mid-stiched	Planmeca Oy (Helsinki, Finland)	16 × 16	90	(108, 127, 145) 271, **325**, 380 "361, 433, 506"	(95, 112, 128) 223, **283**, 339 "304, 365, 426"	**345**	1428	235	145	2436	345	5049	189	Current study
SkyView®	Cefla Dental Group (Imola, Italy)	17 × 17	90	51.5	87	134	125	58	–	719	474	1582	224	Pauwels et al[30]
iCAT NG	Imaging Sciences (Hatfield, PA)	17 × 23	120	18.7	46	40	160	60	20	660	50	850	86	Morant et al[21]
3D eXam®	Imaging Sciences	17 × 23	120	37	156	–	–	–	–	–	–	–	–	Rottke et al[31]
3D eXam	Imaging Sciences	17 × 23	120	**18.5**	**72**	–	–	–	–	–	–	–	–	Schilling and Geibel[32]
iCAT® FLX	Imaging Sciences	17 × 23	120	**18.5**, 37	**69**, 136	**84**	**202**	**50**	**39**	**668**	**301**	**1293**	**195**	Ludlow and Walker[22]
iCAT NG	Imaging Sciences	17 × 23	120	**18.5**, 37	**67**[a], 129	**139**	**277**	**39**	**15**	**888**	**159**	**1158**	**165**	Grunheid et al[33]
iCAT NG	Imaging Sciences	17 × 23	120	**18.5**	**74**	**147**	**294**	**52**	**33**	**950**	**183**	**1250**	**186**	Ludlow and Ivanovic[15]
iCAT NG	Imaging Sciences	17 × 23	120	**18.5**	**78**	–	–	–	–	–	–	–	–	Davies et al[34]
iCAT NG	Imaging Sciences	17 × 23	120	37	182	–	–	–	–	–	–	–	–	Roberts et al 2009[35]
Alphard VEGA	Asahi Roentgen (Kyoto, Japan)	18 × 20	80	68, **102**	123, **183**	**427**	**1982**	**292**	**28**	**1530**	**533**	**4090**	**532**	Kim et al[36]
CS 9500	Carestream Dental (Atlanta, GA)	18 × 20	90	**108**	**136**	**206**	**215**	**92**	–	**1205**	**585**	**2676**	**380**	Pauwels et al[30]
CS 9500	Carestream Dental	18 × 20	80, **85**, 90	86.4, **108**, 108	93, **163**, 260	**218**	**747**	**123**	**131**	**1640**	**835**	**2645**	**389**	Ludlow[10]
CS 9500	Carestream Dental	18 × 20	90	**108**	**151**	–	–	–	–	–	–	–	–	Rottke et al[31]
CB Mercuray	Hitachi (Tokyo, Japan)	19 × 19	**100**, 120	**100**, 150	**569**, 1073	**692**	**3211**	**389**	**393**	**3967**	**6333**	**5467**	**828**	Ludlow and Ivanovic[15]
CB Mercuray	Hitachi	19 × 19	120[b]	150[b]	916	1726	8019	846	365	10,100	3200	13,900	1976	Librizzi et al[37]
CB Mercuray	Hitachi	19 × 19	80, **100**, 100, 120	100, **100**, 150, 150	256, **466**, 683, 932	–	–	–	–	–	–	–	–	Jadu et al[38]
Iluma	Imtec (Ardmore, OK)	19 × 19	120[b]	76, **152**	94, **157**	–	–	–	–	–	–	–	–	Vassileva and Stoyanov[16]
Ilumina	Imtec	19 × 19	120	**20**	**98**	**161**	**745**	**82**	**50**	**1267**	**350**	**1661**	**248**	Ludlow and Ivanovic[15]
Ilumina	Imtec	19 × 19	120[b]	152[b]	498	834	3869	421	233	6267	1733	8400	1265	Ludlow and Ivanovic[15]
NewTom 3G	Cefla Dental Group	19 × 19	110	**8.1**	**68**	**125**	**581**	**62**	**57**	**700**	**333**	**956**	**140**	Ludlow and Ivanovic[15]
NewTom 9000	Cefla Dental Group	19 × 19	110	Auto	95	78	190	60	60	180	775	1550	273	Qu et al[39]
DCT PRO	VATECH (Seoul, Korea)	19 × 20	90	105	254	**391**	1260	160	143	**1740**	**1895**	**3210**	**518**	Qu et al[40]

H, height; kVp, kilovolt peak; mAs, milliampere per second; W, width.
Bold values represent parameters used to produce standard or default scans.
[a]Average of 0.3 and 0.4 voxel scan data.
[b]Initial manufacturer recommended exposure—subsequently reduced.

Table 4 Adult phantom equivalent and effective doses for standard or default exposures for medium field of view (FOV) CBCT units (10–15 cm height)

Unit name	*Manufacturer*	*FOV size* H × W *(cm)*	*kVp*	*mAs*	*Effective dose (μSv)*	*Bone marrow (μSv)*	*Bone surface (μSv)*	*Skin (μSv)*	*Oesophagus (μSv)*	*Brain (μSv)*	*Thyroid (μSv)*	*Salivary glands (μSv)*	*Remainder (μSv)*	*Study*
3D Accuitomo 170	J Morita (Osaka, Japan)	10 × 10	90	45, 79, **87.5**, 154	132, 232, **257**, 453	**267**	**831**	**152**	**140**	**176**	**1498**	**5487**	**776**	Current study
Alphard VEGA	Asahi Roentgen (Kyoto, Japan)	10 × 10	80	68, **136**	85, **184**	**217**	**1009**	**147**	**43**	**496**	**872**	**6233**	**788**	Kim et al[36]
CB Mercuray	Hitachi (Tokyo, Japan)	10 × 10	**120**	**150**	**407**	**466**	**2161**	**344**	**110**	**2950**	**1300**	**9006**	**1355**	Ludlow and Ivanovic[15]
CB Mercuray	Hitachi	10 × 10	80, 100, **120**	100, 100, **150**	148, 261, **421**	–	–	–	–	–	–	–	–	Jadu et al[38]
Alphard VEGA	Asahi Roentgen	10 × 10	80	68, **136**	69, **146**	**196**	**907**	**308**	**17**	**1019**	**403**	**4544**	**659**	Kim et al[36]
CB Mercuray	Hitachi	10 × 10	80, 100, **120**	100, 100, **150**	60, 97, **145**	–	–	–	–	–	–	–	–	Jadu et al[38]
CS 9300	Carestream Dental (Atlanta, GA)	10 × 10	90	**25**	**76**	**57**	**208**	**44**	**37**	**123**	**359**	**1855**	**257**	Current study
3D Accuitomo 170	J Morita	10 × 14	90	45, 79, **87.5**, 154	138, 242, **269**, 473	**286**	**897**	**171**	**150**	**292**	**1372**	**5861**	**843**	Current study
3D Accuitomo 170	J Morita	10 × 14	90	87.5	188	–	–	–	–	–	–	–	–	Theodorakou et al[41]
NewTom VG	QR (Verona, Italy)	10 × 15	110	10.4	83	**115**	**163**	**50**	–	**251**	**354**	**1690**	**281**	Pauwels et al[30]
iCAT NG	Imaging Sciences (Hatfield, PA)	10 × 16	120	10, **18.5**	32, **53**	**30**	**120**	**50**	**40**	**190**	**70**	**1150**	**98**	Morant et al[21]
DCT PRO	VATECH (Seoul, Korea)	10 × 16	90	105	249	**170**	**550**	**110**	**165**	**290**	**2700**	**3780**	**556**	Qu et al[40]
NewTom VG	Cefla Dental Group (Imola, Italy)	11 × 15	110	Auto	81	–	–	–	–	–	–	–	–	Theodorakou et al[41]
iCAT NG	Imaging Sciences	11 × 16	120	10, **18.5**	36, **58**	**40**	**150**	**60**	**40**	**310**	**80**	**1230**	**110**	Morant et al[21]
iCAT® FLX	Imaging Sciences	11 × 16	90/ **120**	6/10, **18.5**, 37	9/43, **79**, 159	**79**	**176**	**41**	**43**	**238**	**353**	**1859**	**256**	Ludlow and Walker[22]
CS 9300	Carestream Dental	11 × 17	90	25.6, **51.5**	101, **204**	**210**	**735**	**158**	**116**	**820**	**930**	**4445**	**626**	Current study
NewTom VGi	QR	12 × 15	110	**6.2**	**103**	**100**	**269**	**113**	**54**	**878**	**477**	**2076**	**301**	Current study
3D Accuitomo 170	J Morita	12 × 17	90	45, 79, **87.5**, 154	154, 260, **325**, 532	**330**	**1052**	**295**	**200**	**446**	**1951**	**5843**	**894**	Current study
3D Accuitomo 170	J Morita	12 × 17	90	87.5	216	–	–	–	–	–	–	–	–	Theodorakou et al[41]
OP300 Maxio	Instrumentarium (Helsinki, Finland)	13 × 15	90	29, 36, **45**, 72	66, 82, **102**, 164	122	414	72	52	180	427	2096	**342**	Current study
i-CAT Classic	Imaging Sciences	13 × 16	120	18.5	**69**	**95**	**1450**	**149**	**30**	**567**	**267**	**1450**	**53**	Ludlow and Ivanovic[15]
iCAT NG	Imaging Sciences	13 × 16	120	18.5	**87**	**105**	**211**	**82**	**45**	**808**	**283**	**1836**	**67**	Ludlow and Ivanovic[15]
iCAT NG	Imaging Sciences	13 × 16	120	10, **18.5**	40, **66**	**50**	**200**	**80**	**40**	**590**	**80**	**1270**	**123**	Morant et al[21]

Table 4. Continued

Unit name	*Manufacturer*	*FOV size* H × W *(cm)*	*kVp*	*mAs*	*Effective dose (μSv)*	*Bone marrow (μSv)*	*Bone surface (μSv)*	*Skin (μSv)*	*Oesophagus (μSv)*	*Brain (μSv)*	*Thyroid (μSv)*	*Salivary glands (μSv)*	*Remainder (μSv)*	*Study*
iCAT NG	Imaging Sciences	13 × 16	120	18.5	83	**116**	**124**	**54**	–	**375**	**355**	**1830**	**260**	Pauwels et al[30]
3D eXam®	Imaging Sciences	13 × 16	120	18.5	107	–	–	–	–	–	–	–	–	Schilling and Geibel[32]
iCAT FLX	Imaging Sciences	13 × 16	90/ **120**	6/10, **18.5**, 37	11/54, **85**, 171	**85**	**185**	**74**	**48**	**380**	**405**	**1898**	**265**	Ludlow and Walker[22]
iCAT NG	Imaging Sciences	13 × 16	120	**18.5**	**77**	–	–	–	–	–	–	–	–	Davies et al[34]
iCAT NG	Imaging Sciences	13 × 16	120	18.5	111	–	–	–	–	–	–	–	–	Roberts et al[35]
iCAT NG	Imaging Sciences	13 × 16	120	18.5	82	–	–	–	–	–	–	–	–	Theodorakou et al[41]
SCANORA® 3D	Soredex (Helsinki, Finland)	13.5 × 14.5	85	48	68	**86**	**94**	**55**	–	**255**	**296**	**1568**	**221**	Pauwels et al[30]
CS 9300	Carestream Dental	13.5 × 17	90	**45.2**	**184**	**159**	**572**	**150**	**103**	**789**	**907**	**4006**	**575**	Current study
Iluma Elite	Imtec (Ardmore, OK)	14 × 21	120	76	368	**660**	**667**	**277**	–	**3415**	**1230**	**7225**	**1034**	Pauwels et al[30]
Alphard VEGA	Asahi Roentgen	15 × 15	80	85, **153**	158, **288**	**609**	**2827**	**421**	**36**	**2834**	**821**	**6931**	**892**	Kim et al[36]
CB Mercuray	Hitachi	15 × 15[a]	120	150	548	874	5110	569	100	8950	1075	8760	**337**	Librizzi et al[37]
CB Mercuray	Hitachi	15 × 15[a]	120	150	560	**940**	**4360**	**641**	**177**	**5933**	**1700**	**10,561**	**379**	Ludlow and Ivanovic[15]
CB Mercuray	Hitachi	15 × 15[a]	100	96	227	485	487	225	50	3032	473	3673	**586**	Lukat et al[42]
CB Mercuray	Hitachi	15 × 15[a]	80, 100, **120**	100, 100, **150**	153, 275, **435**	–	–	–	–	–	–	–	–	Jadu et al[38]
Galileos Comfort	Sirona Dental Systems (Bensheim, Germany)	15 × 15[a]	85	**21**, 42	**70**, 128	**82**	**382**	**40**	**37**	**267**	**233**	**1606**	**57**	Ludlow and Ivanovic[15]
Galileos Comfort	Sirona Dental Systems	15 × 15[a]	85	28	84	**82**	**83**	**55**	–	**124**	**380**	**2104**	**292**	Pauwels et al[30]
Galileos Comfort	Sirona Dental Systems	15 × 15[a]	85	**21**, 42	**51**, 95	–	–	–	–	–	–	–	–	Rottke et al[31]
Galileos Comfort Plus	Sirona Dental Systems	15 × 15[a]	98	8, **10**, 12 (20, 25, 30)	38, **47**, 56 (106, 130, 154)	**43**	**135**	**35**	**29**	**165**	**245**	**1011**	**144**	Current study
NewTom VGi	QR	15 × 15	110	**7.8**	**97**	**107**	**299**	**101**	**51**	**1002**	**440**	**1852**	**269**	Current study
NewTom VGi	QR	15 × 15	110	**8.8**	**194**	**186**	**184**	**98**	–	**605**	**2045**	**2855**	**436**	Pauwels et al[30]

H, height; kVp, kilovoltage peak; mAs, milliampere per second; W, width.
Bold values represent parameters used to produce standard or default scans.
[a]Spherical FOV.

Table 5 Adult phantom equivalent and effective doses for standard or default exposures for small field of view (FOV) CBCT units (<10 cm height) maxillary views

Unit name	*Manufacturer*	*FOV size* H × W *(cm)*	*kVp*	*mAs*	*Effective dose (μSv)*	*Bone marrow (μSv)*	*Bone surface (μSv)*	*Skin (μSv)*	*Oesophagus (μSv)*	*Brain (μSv)*	*Thyroid (μSv)*	*Salivary glands (μSv)*	*Remainder (μSv)*	*Study*
Veraviewepocs 3D	J Morita (Osaka, Japan)	4 × 4[a]	80	**47.5**	**21**	–	**65**	**17**	–	**1**	**1**	**1890**	–	Al-Okshi et al[43]
3D Accuitomo 170	J Morita	4 × 4[a]	90	**87.5**	**32**	–	–	–	–	–	–	–	–	Theodorakou et al[41]
CS 9000	Carestream Dental (Atlanta, GA)	4 × 5[a]	70	**107**	**5**	**5**	**22**	**47**	–	**30**	–	**130**	**20**	Current study
CS 9000	Carestream Dental	4 × 5[b]	70	**107**	**10**	**12**	**49**	**41**	**2**	**60**	–	**220**	**38**	Current study
CS 9000	Carestream Dental	4 × 5[a]	70	**107**	**19**	**21**	**27**	**25**	–	**18**	**30**	**523**	**74**	Pauwels et al[30]
CS 9000	Carestream Dental	4 × 5[a]	70	**85.6**	**24**	–	–	–	–	–	–	–	–	Theodorakou et al[41]
ProMax 3D[c]	Planmeca Oy (Helsinki, Finland)	4 × 5[a]	84	**120**	**10**	–	**40**	**12**	–	**1**	**13**	**650**	–	Al-Okshi et al[43]
3D eXam®	Kavo (Bieberach, Germany)	4 × 16	120	**18.5**, 37	**33**, 68	–	–	–	–	–	–	–	–	Schilling and Geibel[32]
Alphard VEGA	Asahi Roentgen (Kyoto, Japan)	5 × 5[a]	80	102, **153**	20, **22**	**43**	**199**	**73**	**3**	**115**	**99**	**364**	**98**	Kim et al[36]
Alphard VEGA	Asahi Roentgen	5 × 5[b]	80	102, **153**	20, **25**	**41**	**192**	**133**	**6**	**169**	**104**	**494**	**105**	Kim et al[36]
CS 9300	Carestream Dental	5 × 5[a]	84	60, **100**	35, **59**	**40**	**170**	**13**	**15**	**56**	**146**	**1884**	**219**	Current study
CS 9300	Carestream Dental	5 × 5[b]	84	60, **100**	48, **80**	**65**	**290**	**14**	**21**	**80**	**191**	**2399**	**303**	Current study
OP300 Maxio	Instrumentarium (Helsinki, Finland)	5 × 5[a]	90	11.7, 14.7, **18.7**, 23.4	12, 16, **20**, 25	**40**	**128**	**17**	**5**	**20**	**42**	**318**	**68**	Current study
PaX-Uni3D	VATECH (Seoul, Korea)	5 × 5[a]	85	120	44	**47**	**49**	**55**	–	**28**	**209**	**1073**	**146**	Pauwels et al[30]
Orthophos XG	Sirona Dental Systems (Bensheim, Germany)	5 × 5.5[a]	85	36, **51**, 66, (72, 86, 101)	21, **30**, 39, (45, 53, 60)	**26**	**120**	**16**	**8**	**28**	**76**	**896**	**108**	Current study
Orthophos XG	Sirona Dental Systems	5 × 5.5[b]	85	36, **51**, 66, (72, 86, 101)	25, **36**, 47, (58, 70, 81)	**33**	**156**	**18**	**10**	**31**	**90**	**1036**	**131**	Current study
ProMax 3D[c]	Planmeca Oy	5 × 8	84	192	131	**98**	**341**	**70**	**19**	**86**	**333**	**3865**	**514**	Qu et al[19]
3D Accuitomo 170	J Morita	5 × 10	90	87.5	54	**112**	**112**	**62**	–	**189**	**148**	**2138**	**85**	Pauwels et al[30]
3D Accuitomo 170	J Morita	5 × 10	90	45, 79, **87.5**, 154	58, 102, **113**, 198	**224**	**668**	**102**	**27**	**147**	**249**	**1951**	**382**	Current study
CS 9300	Carestream Dental	5 × 10	90	25	56	**36**	**141**	**8**	**13**	**52**	**116**	**1264**	**171**	Current study
3D Accuitomo 170	J Morita	5 × 14	90	45, 79, **87.5**, 154	70, 123, **136**, 240	**256**	**767**	**106**	**34**	**201**	**299**	**2477**	**474**	Current study
3D Accuitomo 170	J Morita	5 × 14	90	87.5	70	–	–	–	–	–	–	–	–	Theodorakou et al[41]
3D Accuitomo 170	J Morita	5 × 17	90	45, 79, **87.5**, 154	68, 119, **132**, 232	**240**	**721**	**85**	**36**	**205**	**298**	**2452**	**460**	Current study
Pan eXam Plus 3D	Kavo	6 × 4	90	23, 49	40, 79	–	–	–	–	–	–	–	–	Schilling and Geibel[32]
3D Accuitomo 170	J Morita	6 × 6[a]	90	27, 45, 52.5, 79, **87.5**, 154	19, 32, 37, 56, **62**, 109	**107**	**325**	**107**	**18**	**104**	**163**	**1126**	**210**	Current study
3D Accuitomo 170	J Morita	6 × 6[b]	90	27, 45, 52.5, 79, **87.5**, 154	20, 33, 39, 58, **65**, 114	**104**	**326**	**78**	**15**	**123**	**140**	**1068**	**250**	Current study

Table 5. Continued

Unit name	*Manufacturer*	*FOV size* H × W *(cm)*	*kVp*	*mAs*	*Effective dose (μSv)*	*Bone marrow (μSv)*	*Bone surface (μSv)*	*Skin (μSv)*	*Oesophagus (μSv)*	*Brain (μSv)*	*Thyroid (μSv)*	*Salivary glands (μSv)*	*Remainder (μSv)*	*Study*
NewTom VGi	QR (Verona, Italy)	6 × 6[b]	110	70.1	140	**191**	**486**	**101**	**47**	**1028**	**355**	**2763**	**478**	Current study
NewTom VGi	QR	6 × 6[a]	110	65	131	**173**	**442**	**132**	**42**	**982**	**332**	**2612**	**443**	Current study
OP300 Maxio	Instrumentarium	6 × 8	90	11.7, 14.7, **18.7**, 23.4	25, 31, **40**, 50	**87**	**275**	**27**	**9**	**46**	**79**	**621**	**134**	Current study
Pan eXam Plus 3D	Kavo	6 × 8	90	47, 79	79, 125	–	–	–	–	–	–	–	–	Schilling and Geibel[32]
iCAT® FLX	Imaging Sciences (Hatfield, PA)	6 × 16	90/ **120**	6/10, **18.5**, 37	4/20, **32**, 65	**32**	**73**	**11**	**12**	**131**	**101**	**719**	**119**	Ludlow and Walker[22]
iCAT NG	Imaging Sciences	6 × 16	120	**18.5**, 37	**32**, 60	–	–	–	–	–	–	–	–	Davies et al[34]
iCAT NG	Imaging Sciences	6 × 16	120	10, **18.5**	22, **35**	–	–	–	–	–	–	–	–	Morant et al[21]
iCAT NG	Imaging Sciences	6 × 16	120	**18.5**, 37	**37**, 68	–	–	–	–	–	–	–	–	Roberts et al[35]
iCAT NG	Imaging Sciences	6 × 16	120	**18.5**	**33**	–	–	–	–	–	–	–	–	Theodorakou et al[41]
iCAT NG	Imaging Sciences	8 × 16	120	10, **18.5**	29, **47**	–	–	–	–	–	–	–	–	Morant et al[21]
SCANORA® 3D	Soredex (Helsinki, Finland)	7.5 × 10	85	**30**	**46**	**42**	**50**	**30**	–	**45**	**148**	**1285**	**178**	Pauwels et al[30]
Galileos Comfort Plus	Sirona Dental Systems	8.5 × 15	98	8, **10**, 12 (20, 25, 30)	27, **34**, 41 (84, 103, 122)	**41**	**127**	**34**	**13**	**164**	**103**	**869**	**118**	Current study
Alphard VEGA	Asahi Roentgen	10 × 10	80	68, **136**	69, **146**	**196**	**907**	**308**	**17**	**1019**	**403**	**4544**	**659**	Kim et al[36]
CB Mercuray	Hitachi (Tokyo, Japan)	10 × 10	80, 100, **120**	100, 100, **150**	60, 97, **145**	–	–	–	–	–	–	–	–	Jadu et al[38]

H, height; kVp, kilovoltage peak; mAs, milliampere per second; W, width.
Bold values represent parameters used to produce standard or default scans.
[a]Anterior.
[b]Posterior.
[c]Upgraded unit with additional filtration.

Table 6 Adult phantom effective doses for standard or default exposures for small field of view (FOV) CBCT units (<10 cm height) views including mandible

Unit name	*Manufacturer*	*FOV size* H × W *(cm)*	*kVp*	*mAs*	*Effective dose (μSv)*	*Bone marrow (μSv)*	*Bone surface (μSv)*	*Skin (μSv)*	*Oesophagus (μSv)*	*Brain (μSv)*	*Thyroid (μSv)*	*Salivary glands (μSv)*	*Remainder (μSv)*	*Study*
3D Accuitomo 170	J Morita (Osaka, Japan)	4 × 4[a]	90	**87.5**	**43**	**37**	**37**	**32**	–	37	195	2120	70	Pauwels et al[30]
Veravieweposcs 3D	J Morita	4 × 4[a]	80	**47**	**22**	**36**	**108**	**15**	–	–	**50**	**900**	–	Al-Okshi et al[43]
CS 9000	Carestream Dental (Atlanta, GA)	4 × 5[b]	70	**107**	**22**	**21**	**85**	**42**	**4**	**20**	**40**	**633**	**80**	Current study
CS 9000	Carestream Dental	4 × 5[a]	70	**107**	**40**	**78**	**35**	**24**	–	**290**	**251**	**709**	**86**	Pauwels et al[30]
CS 9000	Carestream Dental	4 × 5[a]	70	**107**	**38**	**37**	**150**	**10**	**10**	**20**	**110**	**1037**	**141**	Current study
3D eXam®	Kavo (Bieberach, Germany)	4 × 16	120	**18.5**, 37	**38**, 76	–	–	–	–	–	–	–	–	Schilling and Geibel[32]
Alphard VEGA	Asahi Roentgen (Kyoto, Japan)	5 × 5	80	102, **153**	62, **94**	**95**	**442**	**131**	**17**	**75**	**316**	**3570**	**507**	Kim et al[36]
CS 9300	Carestream Dental	5 × 5[b]	84	60, **100**	48, **81**	**56**	**207**	**44**	**37**	**32**	**424**	**2350**	**243**	Current study
CS 9300	Carestream Dental	5 × 5[a]	84	60, **100**	66, **127**	**87**	**332**	**54**	**66**	**51**	**384**	**3220**	**382**	Current study
OP300 Maxio	Instrumentarium (Helsinki, Finland)	5 × 5[b]	90	11.7, 14.7, **18.7**, 23.4	16, 20, **26**, 32	**14**	**52**	**16**	**15**	**8**	**162**	**621**	**83**	Current study
Orthophos XG	Sirona Dental Systems (Bensheim, Germany)	5 × 5.5[b]	85	36, **51**, 66 (72, 86, 101)	22, **31**, 40 (49, 65, 84)	**24**	**101**	**17**	**16**	**16**	**160**	**850**	**92**	Current study
Orthophos XG	Sirona Dental Systems	5 × 5.5[a]	85	36, **51**, 66 (72, 86, 101)	27, **38**, 50, (61, 72, 83)	**33**	**142**	**19**	**21**	**19**	**207**	**951**	**116**	Current study
ProMax 3D[c]	Planmeca Oy (Helsinki, Finland)	5 × 8	84	192	171	**95**	**329**	**38**	**60**	**20**	**855**	**4048**	**659**	Qu et al[19]
3D Accuitomo 170	J Morita	5 × 10	90	45, 79, **87.5**, 154	87, 153, **169**, 297	**86**	**294**	**41**	**112**	**43**	**1216**	**4206**	**497**	Current study
CS 9300	Carestream Dental	5 × 10	90	25	75	**58**	**206**	**30**	**38**	**32**	**386**	**1910**	**248**	Current study
3D Accuitomo 170	J Morita	5 × 14	90	45, 79, **87.5**, 154	135, 237, **262**, 461	**258**	**810**	**64**	**127**	**74**	**1226**	**6363**	**865**	Current study
3D Accuitomo 170	J Morita	5 × 17	90	45, 79, **87.5**, 154	121, 212, **235**, 414	**193**	**618**	**62**	**152**	**65**	**1374**	**5539**	**734**	Current study
Pan eXam Plus 3D	Kavo	6 × 4	90	23, 49	49, 115	–	–	–	–	–	–	–	–	Schilling and Geibel[32]
3D Accuitomo 170	J Morita	6 × 6	90	27, 45, 52.5, 79, **87.5**, 154	37, 61, 72, 108, **120**, 210	**111**	**347**	**36**	**54**	**36**	**650**	**2814**	**381**	Current study
3D Accuitomo 170	J Morita	6 × 6	90	27, 45, 52.5, 79, **87.5**, 154	48, 80, 93, 148, **158**, 252	**156**	**514**	**44**	**75**	**55**	**745**	**3150**	**572**	Current study
NewTom VGi	QR (Verona, Italy)	6 × 6	110	**42.1**	**191**	**147**	**381**	**52**	**91**	**258**	**1150**	**4570**	**595**	Current study
NewTom VGi	QR	6 × 6	110	**29**	**130**	**103**	**268**	**72**	**58**	**187**	**667**	**3253**	**426**	Current study

Table 6. Continued

Unit name	*Manufacturer*	*FOV size* H × W *(cm)*	*kVp*	*mAs*	*Effective dose (μSv)*	*Bone marrow (μSv)*	*Bone surface (μSv)*	*Skin (μSv)*	*Oesophagus (μSv)*	*Brain (μSv)*	*Thyroid (μSv)*	*Salivary glands (μSv)*	*Remainder (μSv)*	*Study*
OP300 Maxio	Instrumentarium	6 × 8	90	11.7, 14.7, **18.7**, 23.4	43, 54, **68**, 86	**86**	**282**	**28**	**33**	**18**	**305**	**1523**	**221**	Current study
Pan eXam Plus 3D	Kavo	6 × 8	90	47, 79	110, 184	–	–	–	–	–	–	–	–	Schilling and Geibel[32]
iCAT® FLX	Imaging Sciences (Hatfield, PA)	6 × 16	90/ **120**	6/10, **18.5**, 37	8/34, **61**, 127	**61**	**124**	**18**	**33**	**51**	**290**	**1567**	**198**	Ludlow and Walker[22]
iCAT NG	Imaging Sciences	6 × 16	120	18.5	45	**33**	**33**	**25**	–	**46**	**251**	**973**	**172**	Pauwels et al[30]
iCAT NG	Imaging Sciences	6 × 16	120	**18.5**, 37	**58**, 113	–	–	–	–	–	–	–	–	Davies et al[34]
iCAT NG	Imaging Sciences	6 × 16	120	10, **18.5**	24, **39**	–	–	–	–	–	–	–	–	Morant et al[21]
iCAT NG	Imaging Sciences	6 × 16	120	**18.5**, 37	**75**, 149	–	–	–	–	–	–	–	–	Roberts et al[35]
iCAT NG	Imaging Sciences	6 × 16	120	18.5	49	–	–	–	–	–	–	–	–	Theodorakou et al[41]
Picasso Trio	VATECH (Seoul, Korea)	7 × 12	85	91	81	62	**57**	56	–	39	583	1837	**254**	Pauwels et al[30]
Picasso Trio	VATECH	7 × 12	85	91, 127, (**109**)[d]	81, 123, (**102**)[d]	**94**	**107**	**85**	–	**87**	**567**	**2410**	**342**	Pauwels et al[30]
Picasso Trio	VATECH	7 × 12	85	127	123	126	**156**	113	–	134	551	2982	**432**	Pauwels et al[30]
DCT PRO	VATECH	7 × 16	90	105	180	76	240	20	150	20	2360	2280	**377**	Qu et al[40]
SCANORA® 3D	Soredex (Helsinki, Finland)	7.5 × 10	85	30	47	**34**	**35**	**29**	–	**25**	**352**	**1052**	**147**	Pauwels et al[30]
SCANORA 3D	Soredex	7.5 × 10	85	30	45	**37**	**39**	**31**	–	**31**	**240**	**1117**	**155**	Pauwels et al[30]
3D Accuitomo 170	J Morita	8 × 8	90	45, 79, **87.5**, 154	92, 162, **180**, 316	**180**	**560**	**103**	**85**	**83**	**921**	**4257**	**564**	Current study
3D eXam	Kavo	8 × 8	120	**18.5**, 37	**62**, 122	–	–	–	–	–	–	–	–	Schilling and Geibel[32]
CS 9300	Carestream Dental	8 × 8	90	**32**	**75**	**59**	**219**	**33**	**32**	**69**	**330**	**1935**	**254**	Current study
iCAT FLX	Imaging Sciences	8 × 8	90/ **120**	6/10, **18.5**, 37	5/23, **44**, 85	**85**	**139**	**23**	**42**	**58**	**222**	**1172**	**149**	Ludlow and Walker[22]
iCAT NG	Imaging Sciences	8 × 8	120	10, **18.5**	18, **29**	–	–	–	–	–	–	–	–	Morant et al[21]
NewTom VGi	QR	8 × 8	110	**6.3** (38.7)	**61** (206)	**53**	**139**	**43**	**26**	**174**	**258**	**1494**	**208**	Current study
OP300 Maxio	Instrumentarium	8 × 8	90	11.7, 14.7, **18.7**, 23.4	49, 61, **78**, 97	**93**	**308**	**35**	**35**	**24**	**335**	**1754**	**255**	Current study
Orthophos XG	Sirona Dental Systems	8 × 8	85	36, **51**, 66 (72, 86, 101)	48, **67**, 91 (117, 144, 166)	53	240	28	32	**53**	**298**	**1718**	**226**	Current study
Prexion 3D high res	TeraRecon (Foster City, CA)	8 × 8	90	148	388	325	1508	264	133	783	1800	9372	**1309**	Ludlow and Ivanovic[15]
Prexion 3D standard	TeraRecon	8 × 8	90	76	189	**164**	**760**	**135**	**53**	**383**	**683**	**4761**	**684**	Ludlow and Ivanovic[15]
ProMax 3D	Planmeca Oy	8 × 8	84	19.6, **169**	28, **122**	**88**	**121**	**145**	–	**53**	**1021**	**2576**	**346**	Pauwels et al[30]
ProMax 3D	Planmeca Oy	8 × 8	84	19.6	18	–	–	–	–	–	–	–	–	Theodorakou et al[41]

Table 6. Continued

Unit name	*Manufacturer*	*FOV size* H × W *(cm)*	*kVp*	*mAs*	*Effective dose (μSv)*	*Bone marrow (μSv)*	*Bone surface (μSv)*	*Skin (μSv)*	*Oesophagus (μSv)*	*Brain (μSv)*	*Thyroid (μSv)*	*Salivary glands (μSv)*	*Remainder (μSv)*	*Study*
Promax 3D	Planmeca Oy	8 × 8	84	**72**, 96	**488**, 652	**468**	**2170**	**339**	**120**	**600**	**1267**	**12 939**	**1846**	Ludlow and Ivanovic[15]
ProMax 3D[c]	Planmeca Oy	8 × 8	84	22.4, 96, 120, 144, **168**, 192, 192	30, 102, 169, 216, **272**, 298, 306	**255**	**883**	**163**	**94**	**215**	**1101**	**6582**	**962**	Qu et al[19]
Veravieweposcs 3D	J Morita	8 × 8	70	51	73	**55**	**57**	**69**	–	**40**	**330**	**1956**	**85**	Pauwels et al[30]
NewTom VGi	QR	8 × 12	110	**6.1**, (39.1)	**82** (280)	**87**	**219**	**49**	**41**	**237**	**316**	**1942**	**275**	Current study
Kodak 9500	Carestream Dental	8 × 15	90	108	92	**85**	**84**	**51**	–	**91**	**541**	**2166**	**304**	Pauwels et al[30]
OP300 Maxio	Instrumentarium	8 × 15	90	22.5, 28.4, **36**, 45	76, 96, **121**, 152	**127**	**431**	**71**	**66**	**58**	**550**	**2680**	**409**	Current study
3D eXam	Kavo	8 × 16	120	10, 37 (**18.5**)	45, 170 (**88**)	–	–	–	–	–	–	–	–	Schilling and Geibel[32]
iCAT FLX	Imaging Sciences	8 × 16	90/ **120**	6/10, **18.5**, 37	8/39, **70**, 148	**70**	**150**	**23**	**40**	**95**	**329**	**1693**	**225**	Ludlow and Walker[22]
iCAT NG	Imaging Sciences	8 × 16	**120**	**18.5**, 37	**65**, 134	**76**	**151**	**33**	**17**	**150**	**183**	**1639**	**235**	Grunheid et al[33]
Galileos Comfort plus	Sirona Dental Systems	8.5 × 15	**98**	8, **10**, 12 (20, 25, 30)	29, **37**, 45, (92, 113, 133)	**40**	**118**	**21**	**26**	**23**	**225**	**894**	**121**	Current study
CS 9500	Carestream Dental	9 × 15	80, **85**, 90	86.4, **108**, 108	76, **98**, 166	**113**	**386**	**55**	**54**	**264**	**533**	**1680**	**313**	Ludlow[10]
Alphard VEGA	Asahi Roentgen	10 × 10	**80**	68, **136**	85, **184**	**217**	**1009**	**147**	**43**	**496**	**872**	**6233**	**788**	Kim et al[36]
CB Mercuray	Hitachi (Tokyo, Japan)	10 × 10	**120**	**150**	**407**	**466**	**2161**	**344**	**110**	**2950**	**1300**	**9006**	**1355**	Ludlow and Ivanovic[15]
CB Mercuray	Hitachi	10 × 10	80, 100, **120**	100, 100, **150**	148, 261, **421**	–	–	–	–	–	–	–	–	Jadu et al[38]

H, height; kVp, kilovoltage peak; mAs, milliampere per second; W, width.
Bold values represent parameters used to produce standard or default scans.
[a]Posterior.
[b]Anterior.
[c]Upgraded unit with additional filtration.
[d]Average of high- and low-dose protocols.

Table 7 Adult phantom equivalent and effective doses for standard or default exposures for small field of view (FOV) CBCT units (<10 cm height)—temporomandibular joint views

Unit name	*Manufacturer*	*FOV size* H × W *(cm)*	*kVp*	*mAs*	*Effective dose (μSv)*	*Bone marrow (μSv)*	*Bone surface (μSv)*	*Skin (μSv)*	*Oesophagus (μSv)*	*Brain (μSv)*	*Thyroid (μSv)*	*Salivary glands (μSv)*	*Remainder (μSv)*	*Study*
CS 9000	Carestream Dental (Atlanta, GA)	4 × 5	68, **70**, 70	68, **86**, 108	10, **14**, 21	18	**18**	–	–	**218**	**23**	**231**	**43**	Lukat et al[42]
NewTom VGi	QR (Verona, Italy)	8 × 8	**110**	**22, 93**	**45**, 129	**40**	**102**	**62**	–	**150**	**20**	**2130**	–	Al-Okshi et al[43]
NewTom VGi	QR	8 × 12	110	**19.1**	56	**48**	**122**	**74**	–	**230**	**20**	**2400**	–	Al-Okshi et al[43]
CB Mercuray	Hitachi (Tokyo, Japan)	10 × 10	120	150	279	244	**1882**	**308**	**53**	**6500**	**538**	4810	**190**	Librizzi et al[37]

H, height; kVp, kilovoltage peak; mAs, milliampere per second; W, width.
Bold values represent parameters used to produce standard or default scans.

doses from standard protocols ranged from 46 to 916 μSv. Table 4 lists doses for medium FOVs. Reported effective doses from standard protocols ranged from 47 to 560 μSv. Tables 5 and 6 provide doses for maxillary and mandibular small FOVs, respectively. Standard protocol doses ranged from 5 to 140 μSv for maxillary views and from 18 to 488 μSv for views including the mandible. Table 7 catalogues temporomandibular joint FOVs. Table 8 combines large and medium FOVs for child phantoms. Doses from standard protocols ranged from 39 to 430 μSv. Tables 9 and 10 list child doses for maxillary and mandibular small FOVs, respectively. Maxillary effective doses from standard protocols ranged from 16 to 177 μSv, while FOVs including the mandible ranged from 24 to 331 μSv. Reported adult effective doses for any protocol in Tables 3–6 ranged from 46 to 1073 μSv for large FOVs, 9–560 μSv for medium FOVs and 5–652 μSv for small FOVs. Child effective doses from any protocol in Tables 7–10 ranged from 13 to 769 μSv for large or medium FOVs and 5–582 μSv for small FOVs. Although standard protocols were the focus of this study, the included reports and additional data provided a total of 41 large FOV protocols, 81 medium FOV protocols and 249 small FOV protocols for adult phantom imaging. For child imaging protocols, the totals were 8, 35 and 103 for large, medium and small FOVs, respectively.

Tables 11–14 provide summary data for adult and child doses and include mean values with standard deviations for standard or default exposure equivalent and effective doses. Lower numbers of units with equivalent doses reflect the practice of some studies that have included fewer weighted tissues in their calculation of effective dose or report only effective dose. Standard adult exposure settings resulting in average adult effective doses of 212 μSv for large FOVs, 177 μSv for medium FOVs and 84 μSv for small FOVs are found in Table 11. Small adult FOVs producing average effective doses of 53 μSv for maxillary views and 102 μSv for mandibular views are seen in Table 12. Because data for few large FOVs were found for child phantoms, large and medium FOVs were combined in Table 13. The average effective dose for large or medium FOVs was 175 μSv. The average child effective dose for small FOVs was 103 μSv. When child phantom small FOVs were analysed by arch location, an average dose of 67 μSv was seen for maxillary views and of 128 μSv was seen for mandibular views, as seen in Table 14.

Table 15 provides *p*-values for an ANOVA of effective dose and equivalent doses for each of the weighted tissues that are typically included in head and neck dosimetry studies. The ANOVA model investigated the effects of FOV and phantom type. Tukey honest significant difference results are provided for FOV for statistically significant factors. With the exception of remainder tissues, all weighted tissues and effective dose demonstrated significantly increased dose with increased FOV size. With the exception of thyroid dose, which was significantly greater in child exposures, no differences

Table 8 Child phantom equivalent and effective doses for standard or default exposures for medium and large field of view (FOV) CBCT units (>10 cm height)

Unit name	*Manufacturer*	*FOV size* H × W *(cm)*	*kVp*	*mAs*	*Effective dose (μSv)*	*Bone marrow (μSv)*	*Bone surface (μSv)*	*Skin (μSv)*	*Oesophagus (μSv)*	*Brain (μSv)*	*Thyroid (μSv)*	*Salivary glands (μSv)*	*Remainder (μSv)*	*Study*
ProMax mid-stiched	Planmeca Oy (Helsinki, Finland)	16 × 16	90	(72.3, 90) **217**, 244 "289, 362"	(88, 107) **277**, 307 "362, 488"	**318**	**1118**	**222**	**112**	**2829**	**2154**	**3706**	**145**	Current study
Iluma	Imtec (Ardmore, OK)	19 × 19	120	20	46	–	–	–	–	–	–	–	–	Vassileva and Stoyanov[16]
Newtom 3G	Cefla Dental Group (Imola, Italy)	20 × 20	110	AEC	**56**	71	182	22	44	430	595	531	85	Current study
3D Accuitomo 170	J Morita (Osaka, Japan)	10 × 10	90	45, 79, **87.5**, 154	160, 281, **311**, 548	**151**	**580**	**354**	**99**	**1141**	**2804**	**5736**	**825**	Current study
CS 9300	Carestream Dental (Atlanta, GA)	10 × 10	80	**25**	**86**	**43**	**187**	**47**	**30**	**171**	**846**	**1489**	**223**	Current study
3D Accuitomo 170	J Morita	10 × 14	**90**	**87.5**	**237**	–	–	–	–	–	–	–	–	Theodorakou et al[41]
3D Accuitomo 170	J Morita	10 × 14	**90**	45, 79, **87.5**, 154	183, 321, **355**, 626	**209**	**804**	**319**	**114**	**1693**	**2993**	**6440**	**947**	Current study
Newtom VG	Cefla Dental Group	11 × 15	**110**	Auto	114	–	–	–	–	–	–	–	–	Theodorakou et al[41]
iCAT® FLX	Imaging Sciences (Hatfield, PA)	11 × 16	90/ **120**	6/10, **18.5**	13, 56, **115**	**115**	**190**	**81**	**53**	**391**	**1001**	**2045**	**302**	Ludlow and Walker[22]
CS 9300	Carestream Dental	11 × 17	**80**	25.6, **41.2**	110, **178**	**120**	**524**	**111**	**81**	**850**	**1648**	**2751**	**425**	Current study
3D Accuitomo 170	J Morita	12 × 17	**90**	87.5	282	–	–	–	–	–	–	–	–	Theodorakou et al[41]
3D Accuitomo 170	J Morita	12 × 17	**90**	45, 79, **87.5**, 154	212, 353, **430**, 769	**244**	**940**	**307**	**253**	**2039**	**4265**	**6622**	**1004**	Current study
OP300 Maxio	Instrumentarium (Helsinki, Finland)	13 × 15	90	**29**, 36, 45, 72	**93**, 108, 134, 215	**58**	**225**	**66**	**38**	**407**	**765**	**1668**	**254**	Current study
iCAT FLX	Imaging Sciences	13 × 16	90/ **120**	6/10, **18.5**	18, 70, **120**	**120**	**211**	**82**	**53**	**731**	**1003**	**2038**	**303**	Ludlow and Walker[22]
iCAT NG	Imaging Sciences	13 × 16	120	18.5	134	–	–	–	–	–	–	–	–	Theodorakou et al[41]
CS 9300	Carestream Dental	13.5 × 17	80	45.2	189	**118**	**509**	**155**	**78**	**964**	**1741**	**3075**	**458**	Current study
Galileos Comfort plus	Sirona Dental Systems (Bensheim, Germany)	15 × 15	98	**6**, 8 (15, 20)	**39**, 52, (122, 160)	26	91	25	22	**185**	**384**	**589**	**91**	Current study
Newtom 3G	Cefla Dental Group	15 × 15	110	Auto	94	100	265	56	44	679	875	1250	190	Current study

H, height; kVp, kilovoltage peak; mAs, milliampere per second; W, width.
Bold values represent parameters used to produce standard or default scans.

Table 9 Child phantom equivalent and effective doses for standard or default exposures for small field of view (FOV) CBCT units (<10 cm height) maxillary views

Unit name	*Manufacturer*	*FOV size* H × W *(cm)*	*kVp*	*mAs*	*Effective dose (μSv)*	*Bone marrow (μSv)*	*Bone surface (μSv)*	*Skin (μSv)*	*Oesophagus (μSv)*	*Brain (μSv)*	*Thyroid (μSv)*	*Salivary glands (μSv)*	*Remainder (μSv)*	*Study*
3D Accuitomo 170	J Morita (Osaka, Japan)	4 × 4[a]	90	87.5	28	–	–	–	–	–	–	–	–	Theodorakou et al[41]
CS 9000	Carestream Dental (Atlanta, GA)	4 × 5[a]	70	85.6	16	–	–	–	–	–	–	–	–	Theodorakou et al[41]
CS 9300	Carestream Dental	5 × 5[a]	75	48, **80**	41, **63**	**26**	**118**	**36**	**12**	**70**	**227**	**1930**	**243**	Current study
CS 9300	Carestream Dental	5 × 5[b]	75	48, **80**	47, **79**	**38**	**172**	**33**	**19**	**62**	**384**	**2165**	**282**	Current study
OP300 Maxio	Instrumentarium (Helsinki, Finland)	5 × 5[a]	90	**11.7**, 14.7, 18.7, 23.4	**16**, 20, 26, 32	**6**	**21**	**20**	**3**	**44**	**53**	**438**	**67**	Current study
3D Accuitomo 170	J Morita	5 × 10	90	45, 79, **87.5**, 154	58, 102, **113**, 198	**44**	**163**	**228**	**26**	**355**	**423**	**2988**	**433**	Current study
CS 9300	Carestream Dental	5 × 10	80	**25**	**45**	**18**	**80**	**27**	**9**	**78**	**161**	**1269**	**179**	Current study
3D Accuitomo 170	J Morita	5 × 14	90	45, 79, **87.5**, 154	85, 149, **165**, 290	**65**	**244**	**245**	**37**	**564**	**568**	**4423**	**648**	Current study
3D Accuitomo 170	J Morita	5 × 17	90	45, 79, **87.5**, 154	91, 160, **177**, 312	**77**	**289**	**177**	**39**	**508**	**575**	**4974**	**701**	Current study
3D Accuitomo 170	J Morita	6 × 6[b]	90	27, 45, 52.5, 79, **87.5**, 154	32, 53, 61, 92, **102**, 180	**37**	**138**	**201**	**21**	**531**	**343**	**2580**	**406**	Current study
OP300 Maxio	Instrumentarium	6 × 8	90	**11.7**, 14.7, 18.7, 23.4	**27**, 34, 43, 54	**9**	**34**	**39**	**5**	**107**	**90**	**708**	**108**	Current study
iCAT® FLX	Imaging Sciences (Hatfield, PA)	6 × 16	90/ **120**	6/10, **18.5**	5, 23, **39**	**39**	**43**	**69**	**11**	**252**	**158**	**889**	**142**	Ludlow and Walker[22]
iCAT NG	Imaging Sciences	6 × 16	**120**	**18.5**	**43**	–	–	–	–	–	–	–	–	Theodorakou et al[41]
Galileos Comfort plus	Sirona Dental Systems (Bensheim, Germany)	8.5 × 15	**98**	**6**, 8 (15, 20)	**21**, 32 (72, 98)	**12**	**41**	**23**	**6**	**175**	**92**	**496**	**72**	Current study

H, height; kVp, kilovoltage peak; mAs, milliampere per second; W, width.
Bold values represent parameters used to produce standard or default scans.
[a]Anterior.
[b]Posterior.

Table 10 Child phantom equivalent and effective doses for standard or default exposures for small field of view (FOV) CBCT units (<10 cm height) views including mandible

Unit name	*Manufacturer*	*FOV size* H × W *(cm)*	*kVp*	*mAs*	*Effective dose (μSv)*	*Bone marrow (μSv)*	*Bone surface (μSv)*	*Skin (μSv)*	*Oesophagus (μSv)*	*Brain (μSv)*	*Thyroid (μSv)*	*Salivary glands (μSv)*	*Remainder (μSv)*	*Study*
CS 9300	Carestream Dental	5 × 5[a]	75	48, **80**	44, **64**	**29**	**135**	**29**	**18**	**44**	**332**	**1776**	**223**	Current study
CS 9300	Carestream Dental	5 × 5[b]	75	48, **80**	56, **86**	**41**	**187**	**36**	**23**	**57**	**532**	**2144**	**285**	Current study
OP300 Maxio	Instrumentarium (Helsinki, Finland)	5 × 5[a]	90	**11.7**, 14.7, 18.7, 23.4	**33**, 42, 53, 67	**22**	**86**	**3**	**10**	**17**	**328**	**641**	**82**	Current study
3D Accuitomo 170	J Morita (Osaka, Japan)	5 × 10	90	45, 79, **87.5**, 154	152, 266, **295**, 519	**151**	**591**	**60**	**107**	**127**	**3382**	**5023**	**660**	Current study
CS 9300	Carestream Dental	5 × 10	80	25	61	**30**	**134**	**24**	**20**	**46**	**457**	**1365**	**192**	Current study
3D Accuitomo 170	J Morita	5 × 14	90	87.5	214	–	–	–	–	–	–	–	–	Theodorakou et al[41]
3D Accuitomo 170	J Morita	5 × 14	90	45, 79, **87.5**, 154	152, 267, **296**, 521	**187**	**739**	**70**	**128**	**142**	**3356**	**3356**	**645**	Current study
3D Accuitomo 170	J Morita	5 × 17	90	45, 79, **87.5**, 154	170, 299, **331**, 582	**196**	**773**	**92**	**113**	**186**	**3326**	**5937**	**833**	Current study
3D Accuitomo 170	J Morita	6 × 6[a]	90	27, 45, 52.5, 79, **87.5**, 154	46, 77, 90, 136, **150**, 265	**67**	**259**	**49**	**42**	**137**	**1031**	**3873**	**469**	Current study
3D Accuitomo 170	J Morita	6 × 6[b]	90	27, 45, 52.5, 79, **87.5**, 154	71, 118, 141, 208, **227**, 375	**108**	**419**	**68**	**72**	**202**	**1549**	**5558**	**725**	Current study
OP300 Maxio	Instrumentarium	6 × 8	90	**11.7**, 14.7, 18.7, 23.4	**61**, 77, 97, 122	**34**	**135**	**6**	**17**	**37**	**576**	**1153**	**164**	Current study
iCAT® FLX	Imaging Sciences (Hatfield, PA)	6 × 16	90/ **120**	6/10, **18.5**	9, 43, **73**	**73**	**98**	**34**	**30**	**106**	**530**	**1654**	**224**	Ludlow and Walker[22]
iCAT NG	Imaging Sciences	6 × 16	120	18.5	63	–	–	–	–	–	–	–	–	Theodorakou et al[41]
3D Accuitomo 170	J Morita	8 × 8	90	45, 79, **87.5**, 154	128, 225, **249**, 439	**117**	**454**	**100**	**74**	**324**	**2269**	**5023**	**687**	Current study
CS 9300	Carestream Dental	8 × 8	80	**32**	**82**	**42**	**183**	**30**	**25**	**80**	**780**	**1529**	**219**	Current study
iCAT FLX	Imaging Sciences	8 × 8	90/ **120**	6/10, **18.5**	7, 34, **60**	**60**	**77**	**20**	**20**	**134**	**403**	**1401**	**191**	Ludlow and Walker[22]
OP300 Maxio	Instrumentarium	8 × 8	**90**	**11.7**, 14.7, 18.7, 23.4	**77**, 97, 123, 153	**43**	**167**	**37**	**23**	**186**	**685**	**1416**	**210**	Current study
ProMax 3D	Planmeca Oy (Helsinki, Finland)	8 × 8	**84**	19.6	24	–	–	–	–	–	–	–	–	Theodorakou et al[41]
iCAT FLX	Imaging Sciences	8 × 16	90/ **120**	6/10, **18.5**	12, 50, **85**	**85**	**126**	**39**	**35**	**192**	**659**	**1754**	**248**	Ludlow and Walker[22]
Galileos® ComfortPLUS	Sirona Dental Systems (Bensheim, Germany)	8.5 × 15	**98**	**6**, 8 (15, 20)	**29**, 44, (99, 136)	**20**	**71**	**11**	**20**	**17**	**327**	**404**	**61**	Current study

H, height; kVp, kilovoltage peak; mAs, milliampere per second; W, width.
Bold values represent parameters used to produce standard or default scans.
[a]Anterior.
[b]Posterior.

Table 11 Average equivalent and effective doses (μSv) for an adult using standard exposure settings of dental CBCT units

Field of view size	*Bone marrow*	*Bone surface*	*Skin*	*Oesophagus*	*Brain*	*Thyroid*	*Salivary glands*	*Remainder*	*Effective dose*
Large									
Units reported	16	16	16	14	16	16	16	16	23
Mean	359	1457	189	122	2182	1130	3484	475	212
SD	428	2081	215	125	2601	1616	3465	502	212
Medium									
Units reported	32	32	32	26	32	32	32	32	43
Mean	233	844	163	75	1211	762	3675	442	177
SD	240	1194	153	53	1911	657	2643	325	137
Small									
Units reported	77	79	78	57	78	77	79	74	101
Mean	94	299	62	43	211	413	2259	316	84
SD	81	376	61	38	746	433	2027	295	78

SD, standard deviation.

were seen in equivalent or effective dose owing to phantom type. A separate analysis investigated dose differences related to maxillary or mandibular location for small FOVs for child and adult phantoms. Significantly higher doses were associated with mandibular field positions for the oesophagus, thyroid, salivary gland and remainder tissues as well as effective dose. Once again, only the thyroid tissue demonstrated significantly higher doses in child phantoms than in adult phantoms.

Distribution of mean effective dose components from large FOV CBCT imaging of adult phantoms is displayed graphically in Figure 1. A similar graphic for combined large or medium FOVs is provided for child phantoms in Figure 2. The graphics demonstrate the greater contribution of thyroid exposure to effective dose in the child (37%) than in adult (20%).

Table 16 provides summary statistics for volume DAP and DHP and the ratios of effective dose to each of these values. The coefficient of variation increases with reduction in FOV area or height. The coefficient of variation is consistently lower for *E*/DHP than for *E*/DAP ratios regardless of the FOV size. This suggests that FOV height may be a better predictor of effective dose than FOV area.

Table 17 displays average absolute error between phantom-based calculations of the effective dose and *E*/DAP or *E*/DHP ratios as coefficients for effective dose estimation. The magnitude of error increases as the FOV size is reduced. The average absolute error for all volumes was 35% for *E*/DAP and decreased to 19% for *E*/DHP. This difference was statistically significant ($p < 0.0001$).

Discussion

Reported dosimetry for standard CBCT exposure settings demonstrated significant reductions in effective dose associated with the use of small FOV sizes. While a trend of dose reduction from large to medium FOVs was seen, this was not statistically significant. The absence of a significant dose–FOV relationship is likely related to two factors. Increasing FOV extends anatomic coverage superiorly increasing the amounts of brain and bone coverage with little increase in exposure of other weighted tissues. The resulting proportional increase in effective dose is smaller than that seen when small fields centred on the dentoalveolar area expand both cranially and caudally in medium FOV volumes. The wide range of effective doses produced using standard settings by different CBCT units is another factor affecting the statistical significance of differences that may be present between medium and large FOVs. Standard deviations associated with dose values for these volumes were on the same order as calculated means indicating substantial variability among devices. Although not assessed in detail in this study, exposure variability also increases substantially when one includes the range of protocol options offered by many manufacturers. Doses for the same FOV may have as much as a 15-fold difference between low-dose and high-resolution protocols.[22]

This study has focused on standard or default exposures. These are protocols recommended by the manufacturer of the CBCT unit for imaging of average or typical patients. It should be noted that manufacturers

Table 12 Small field of view (FOV)—average equivalent and effective doses (μSv) for an adult using standard exposure settings of dental CBCT units

FOV location	*Bone marrow*	*Bone surface*	*Skin*	*Oesophagus*	*Brain*	*Thyroid*	*Salivary glands*	*Remainder*	*Effective dose*
Maxilla									
Units reported	25	27	27	20	27	25	27	25	38
Mean	85	236	53	18	153	155	1374	213	53
SD	75	215	40	13	253	104	949	155	38
Mandible									
Units reported	48	48	48	36	47	48	48	47	59
Mean	100	316	61	57	112	569	2745	380	102
SD	84	388	63	41	151	477	2324	337	88

SD, standard deviation.

Table 13 Average equivalent and effective doses (μSv) by field of view (FOV) size for a 10-year-old child using standard exposure settings of dental CBCT units

FOV size	*Bone marrow*	*Bone surface*	*Skin*	*Oesophagus*	*Brain*	*Thyroid*	*Salivary glands*	*Remainder*	*Effective dose*
Large or medium									
Units reported	13	13	13	13	13	13	13	13	18
Mean	130	448	142	79	962	1621	2918	404	175
SD	83	331	119	61	791	1148	2117	319	115
Small									
Units reported	28	28	28	28	28	28	28	28	34
Mean	60	213	65	34	171	843	2388	336	103
SD	50	202	67	33	154	997	1705	238	89

SD, standard deviation.

may change exposures associated with the standard designation over time. Examples of this are seen with Iluma and CB Mercuray devices. Initially, the highest exposure protocols were recommended for these devices. Later, much lower exposure protocols became the recommended "standard". This is reflected in study data from different investigators in Table 3. While marketing materials were changed to reflect updated standard protocols, the effect on selection of imaging parameters by end users is unclear. Differences between recommended use of products and actual clinical application are not new to dental radiology. Continued use of round cones and D-speed film by many dental practitioners in the face of many years of recommendations by the American Dental Association and the National Commission on Radiation Protection and Measurements encouraging the use of rectangular collimation and high-speed receptors is a prominent example.[44,45]

Methodologic errors in dosimetry and effective dose calculation

Regardless of the FOV size, remainder tissues accounted for <10% of the effective dose calculations using ICRP 1990[12] tissue weights.[18] The brain was the only tissue contributing significant dose in the remainder group. Application of ICRP 2007[13] tissue weights resulted in remainder doses contributing 27–42% to effective dose depending on FOV size and location.[18] Studies excluding remainder tissues from their dose calculations significantly underestimate dose, and a number of these were excluded from this report.[46,47] A citation that did not include oral mucosa, which was added to the remainder group in the 2007 ICRP calculation of effective dose was also excluded.[48] The oral mucosa is directly exposed in any maxillofacial CBCT scan and as a component of the remainder group has a tissue weight of 0.0092. This is nearly the tissue weight of the salivary glands (0.01). Similarly, the extrathoracic region is exposed in most dental CBCT scans. Together, the contribution of these tissues to effective dose exceeds that of the oesophagus, skin, bone surface and brain combined and cannot be overlooked in a calculation of stochastic risk.[18]

Sampling is an important component of dosimetry, and the sampling strategy is critical to both internal validity of a dosimetry study and its extensibility to other studies or patient populations. One approach that has been taken is to sample doses over a regularly spaced grid throughout a phantom. This approach requires many dosemeters and results in time consuming and expensive study protocols. An additional complication is that the tissues and organs of particular interest for radiation biology are not uniformly distributed. A uniform grid of dosemeters may not coincide with the location of a tissue of interest. An alternate approach is to place dosemeters only in the weighted tissues used in the calculation of the effective dose. A uniform distribution of dosemeters within the selected tissue is still a resource intensive choice, so efforts to strategically locate dosemeters within a tissue such that the average dose of a limited number of dosemeters reasonably reflects that of a uniform distribution of dosemeters is desirable. We have used this approach in measuring calvarial bone and marrow doses, where a limited number of strategically positioned dosemeters are used to reflect dose to the entire skull. For tissues that are incompletely contained in the maxillofacial area, sampling of the directly exposed portion of the tissue multiplied by the percentage of total tissue that is directly exposed provides

Table 14 Small field of view (FOV)—average equivalent and effective doses (μSv) by arch for a 10-year-old child using standard exposure settings of dental CBCT units

FOV location	*Bone marrow*	*Bone surface*	*Skin*	*Oesophagus*	*Brain*	*Thyroid*	*Salivary glands*	*Remainder*	*Effective dose*
Maxilla									
Units reported	11	11	11	11	11	11	11	11	14
Mean	34	122	100	17	250	279	2078	298	67
SD	23	89	92	13	205	190	1553	223	54
Mandible									
Units reported	17	17	17	17	17	17	17	17	20
Mean	77	273	42	46	120	1207	2589	360	128
SD	57	234	28	38	82	1138	1813	251	101

SD, standard deviation.

Table 15 ANOVA: all volume data models include phantom type and field of view (FOV); small volume data model includes phantom type and arch

p-values	Post hoc *statistical test*	*Model/HSD variable level*	*Bone marrow*	*Bone surface*	*Skin*	*Oesophagus*	*Brain*	*Thyroid*	*Salivary glands*	*Remainder*	*Effective dose*
		Phantom	0.0538	0.1788	0.8268	0.4821	0.6351	**0.0005**	0.7143	0.8926	0.6198
		FOV size	**<0.0001**	**<0.0001**	**<0.0001**	**<0.0001**	**<0.0001**	**0.0004**	**0.008**	0.0868	**<0.0001**
All	Tukey HSD	Large	A	A	A	A	A	A	A	A	A
FOVs	Test	Medium	B	B	A	A	B	A	A B	A	A
		Small	C	C	B	B	C	B	B	B	B
Small		Phantom	0.0406	0.2986	0.6479	0.3281	0.3009	**0.0009**	0.6789	0.7445	0.1706
FOV		FOV location	0.1262	0.1104	0.384	**<0.0001**	0.0779	**<0.0001**	**0.0042**	**0.0198**	**0.0002**

HSD, honestly significant difference.
Bold values indicated statistical significance at $\alpha < 0.05$.
FOV levels not connected by the same letter (A, B, C) are significantly different.

a reasonable estimation of organ dose. This approach is taken with skin, muscle, bone, lymph nodes and oesophagus in our studies.[10,15,17,22,49] Studies that fail to account for body-wide distributions of tissue produce overestimations of equivalent doses for the bone, bone marrow, oesophagus, lymphoid tissue, muscle and skin.[50,51] This error may result in a 10- to 20-fold overestimation of specific organ dose with a concomitant exaggeration of effective dose. The bone marrow, which varies in quantity and distribution by patient age is accorded different percentages for child and adult phantoms.[22] The same dosemeters may be used to calculate bone and bone marrow dose; however, it is important to account for differences in X-ray attenuation efficiency when calculating absorbed doses. The higher effective atomic number of bone leads to increased photoelectric interactions and increased dose to this tissue. Mass attenuation coefficients for bone and soft tissue are available from a variety of sources and are usually calculated using mono-energetic photons beams.[29] Bone/muscle attenuation ratios can be calculated from these data. A linear fit of ratios from 40 to 80 kV is adequate to cover the mean beam energy range produced by CBCT units. In our studies, the effective beam energy of the highly filtered, low ripple, polychromatic beams used for CBCT is estimated to be two-thirds of the peak beam energy. Using this assumption and an equation developed from the linear fit of monochromatic data, bone muscle attenuation ratios from 1.97 for a peak kilovoltage of 120 kVp to 3.63 for 80 kVp are used. Studies that fail to adjust for attenuation differences of the bone and soft tissues may underestimate bone doses by a factor of 2–4×.[30,42] Examining the ratio of the bone to bone marrow doses using the means in Table 11 suggests a range of 3.1–4.1× average underestimation of the bone dose if dosemeter values are not corrected for bone attenuation efficiency. This will lead to a 2–5% underestimation of effective dose depending on the size of the FOV.

Tissues that are completely outside the field of direct exposure are not sampled in our dosimetry protocol. These tissues account for 75% of the weighted tissues in a full body exposure; however, their indirect exposure in maxillofacial examinations accounts for <2% of effective dose.[18,51,52] Although the oesophagus is typically outside the field of direct exposure during CBCT scans, it is potentially exposed to scatter radiation. Because the oesophagus surrounds an open air space, caudally directed scatter photons can extend into the upper oesophageal passage exposing the mucosal walls. For this reason, an organ fraction of 10% is used in calculating oesophageal dose. Because of the oesophagus tissue weight of 0.04 in the calculation of the effective dose, this organ is as or more important than skin dose. Figure 1 suggests that studies that fail to measure oesophageal dose underestimate effective dose by as much as 2%.[30]

While the use of additional dosemeters in indirectly or directly exposed tissues may increase the precision of calculation of organ dose, it does not guarantee an

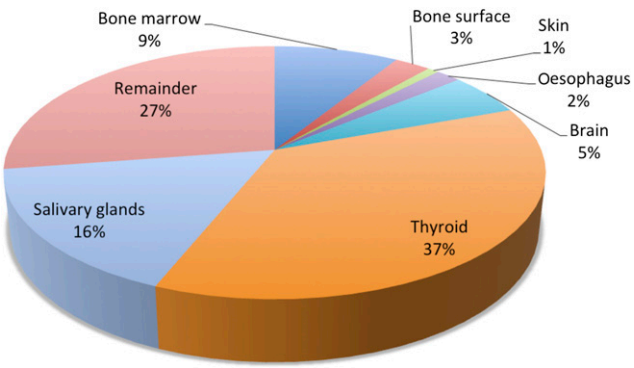

Figure 1 Distribution of effective dose components in an adult phantom for large field of view dental CBCT.

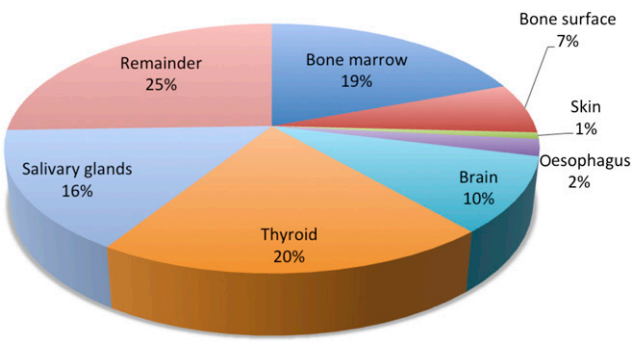

Figure 2 Distribution of effective dose components from large or medium field of view CBCT imaging of a child phantom.

Table 16 Dose–area product (DAP) and dose–volume height (DHP) calculations and derived conversion coefficients for calculating effective dose derived from phantom data

Phantom	*FOV*	*Descriptive statistic*	*DAP (mGy cm²)*	*DHP (mGy cm)*	*Conversion coefficient* E/*DAP* ($\mu Sv\,mGy^{-1}\,cm^{-2}$)	E/*DHP* ($\mu Sv\,mGy^{-1}\,cm^{-1}$)
Adult	Large	Mean	1229	64	0.17	3.44
		SD	1240	66	0.04	0.66
		c.v.	–	–	23%	19%
	Medium	Mean	683	46	0.27	3.90
		SD	574	36	0.08	0.78
		c.v.	–	–	28%	20%
	Small maxilla	Mean	61	7	1.28	8.29
		SD	55	5	0.62	2.66
		c.v.	–	–	48%	32%
	Small mandible	Mean	175	18	0.87	6.63
		SD	161	18	0.51	1.87
		c.v.	–	–	59%	28%
Child	Large and medium	Mean	529	35	0.35	5.07
		SD	362	23	0.10	0.53
		c.v.	–	–	29%	11%
	Small maxilla	Mean	121	11	0.85	6.87
		SD	129	8	0.42	0.74
		c.v.	–	–	49%	11%
	Small mandible	Mean	153	16	1.00	8.47
		SD	126	11	0.43	2.98
		c.v.	–	–	44%	35%

c.v., coefficient of variation; E, effective dose; FOV, field of view; SD, standard deviation.
Analysis by phantom and field of view size.

increase in the accuracy of the calculation of effective dose. Patient positioning for CBCT can vary between devices and operators, and this can have a pronounced effect on dose. Duplication of phantom position when comparing dose differences owing to technique is critical if results are to reflect differences owing to protocol rather than confounding owing to differences in patient position. A 10° rotation in phantom position was noted to produce a 92% difference in dose to the thyroid.[18] Similarly, while caudal–cranial positioning differences of the FOV by a few millimetres may be clinically acceptable, when it results in direct exposure of the thyroid area, it can lead to 3- to 4-fold increases in dose to the thyroid gland and increases in effective dose by as much as 30%.[53]

The allure and disappointment of dose–area product

While the use of DAP has been advocated as a measure of dose for CBCT units,[54,55] its accuracy as a measure of risk is debatable. In relating DAP to effective dose, a conversion coefficient must be used. Using a single CBCT device, a recent study calculated conversion coefficients for DAP to effective dose for large to small FOVs and found that a 3.8-fold range of values (0.038–0.146 $\mu Sv\,mGy^{-1}\,cm^{-2}$) was required for different field sizes and anatomic locations.[36] A 7.5-fold range of *E*/DAP values was calculated from the adult phantom data in this study encompassing a large number of measurements on CBCT devices of varying beam energies. A 2.9-fold range of *E*/DAP values was calculated for a more limited set of child phantom data in this study. The use of volume height in the place of projection area resulted in statistically improved accuracy in the estimation of effective dose but still led to a range in the conversion coefficient of 2.4-fold for adult imaging and a 1.7-fold range for child imaging. A best-case scenario of using conversion factors specific for

Table 17 Absolute error between phantom effective dose and dose calculated with dose–area product (DAP) and dose–height product (DHP) conversion coefficients

Field of view	*Phantom*	n	$E_{phantom} - E_{DAP}$ (μSv)	$E_{phantom} - E_{DHP}$ (μSv)	*Probability* < t
Large	Child	–	–	–	–
	Adult	16	36.4	28.8	**0.0372**
Medium	Child	13	32.5	15.2	**0.0183**
	Adult	32	39.1	27.5	0.0611
Small maxilla	Child	11	41.3	5.1	**0.0213**
	Adult	31	48.2	23.0	**0.0050**
Small mandible	Child	17	45.6	38.7	0.2851
	Adult	48	56.1	25.9	**<0.0001**
All		168	45.7	25.1	**<0.0001**
% diff from *E*		–	35%	19%	–

E, effective dose.
Bold values indicated statistical significance at $\alpha < 0.05$.

FOV size, arch location and patient type still resulted in an average absolute error of 35% of the calculated effective dose when using DAP. Improvement in average absolute error to 19% was seen when volume height was substituted for beam area. This improvement is intriguing as beam height may be easily substituted for beam area in dose calculations. While dose to salivary glands was used in this study, dose measured in air or air kerma are typically used in DAP calculations. These result in different numerical values for effective dose conversion factors but could be hypothesized to provide similar variability for DAP and DHP calculations. While this warrants further investigation, it is apparent that development of universal conversion coefficients to translate simple measures of exposure to patient dose with the goal of risk estimation is problematic.

Why does dose–height product correlate more closely than dose–area product to effective dose?

The dimensions of the rectangular X-ray beam are used to calculate the area portion of DAP. For a homogenous object that is at least the size of the X-ray beam cross section, the product of exposure and beam area will provide a good correlation with absorbed dose. For maxillofacial imaging, the imaged structures are non-homogenous with respect to tissue density, the shape of tissues imaged and the distribution of tissues with respect to radiation sensitivity. Beams of wider width may more than cover the horizontal dimension of the face. The portion of the X-ray beam that extends beyond the face increases beam area but adds negligibly to patient dose because it exposes the patient to only a small amount of scatter photons from the beam interaction with air. The vertical dimensions of even large FOVs rarely exceed the dimension of the maxillofacial area. Therefore, an increase in height of the FOV almost always results in an increased volume of exposed tissue. But DHP is a better correlate with effective dose even for small FOVs. This may be explained by the vertical distribution of radiosensitive organs. Small amounts of direct exposure of an organ contribute more to dose than do larger amounts of scatter radiation. For instance, a small amount of direct exposure of the thyroid gland may result in a dramatic increase in both thyroid and effective dose.[53] Mandibular locations of small FOVs provide greater exposure of the thyroid and submandibular salivary glands than do same size maxillary views. Increasing height of the FOV brings new and potentially radiosensitive tissues into the area of direct exposure, while increasing width of the beam simply increases dose to tissues already being exposed.

Conclusions

Given a choice, dentists prefer images with technical factors that provide high signal-to-noise ratios and high resolution. Dentists requesting images from an imaging centre or providing examinations in their own offices may not understand the risk implications of using higher doses to obtain image volumes. If "pretty pictures" are being obtained when a "just diagnostic" image is needed, we are doing the patient a disservice.[18] As imaging professionals, it is our responsibility to educate our colleagues in other specialities and general dentistry about the risk differences between "diagnostic" and "pretty". This is reason enough for dosimetry research. Recognizing that diagnostic imaging is the single greatest source of exposure to ionizing radiation for the US population that is controllable, the National Commission on Radiation Protection and Measurements has introduced a modification of the as low as reasonably achievable concept. ALADA represents "as low as diagnostically acceptable".[56] Implementation of this concept will require evidence-based judgments of the level of image quality required for specific diagnostic tasks, and exposures and doses associated with this level of quality. Little research is currently available in this area.

For a dosimetry study reporting effective dose to be comparable with the contemporary studies cited in this review, it should incorporate the following elements: the dose calculation should follow the ICRP 2007 recommendations including new and adjusted tissue weights from all weighted tissues in the head and neck area. The location of dosemeters or points of measurement should be specified. When an entire organ is not exposed, such as bone or skin surface, the strategy for extrapolating dose for the entire organ from incomplete sampling should be described. Adjustment for the mass attenuation differences of the bone and soft tissue should be made and described. Adjustments for sensitivity of the dosimetry system for the mean beam energy of the X-ray source should also be described.

Dosimetry research involves many variables in addition to the examination that is being assessed. Decisions affecting these variables may have a profound impact on accuracy, validity and extensibility of results. Currently, anthropomorphic phantom dosimetry, when properly executed, provides the most accurate estimation of effective dose. Large exposure ranges make CBCT doses difficult to generalize. The use of DAP with average conversion coefficients to calculate dose results in significant inaccuracy. The use of DHP as a metric for estimating effective dose improves accuracy and warrants further investigation.

Conflict of interest

Travel support and honoraria were provided to Dr Ludlow by AFP Imaging, Carestream Dental, Instrumentarium, and Sirona Dental Systems. The content is solely the responsibility of the authors and does not necessarily represent the official views of the National Institutes of Health.

References

1. Langland OE, Langlais RP. Early pioneers of oral and maxillofacial radiology. *Oral Surg Oral Med Oral Pathol Oral Radiol Endod* 1995; **80**: 496–511.
2. Rollins W. *Notes on X-light*. Boston, MA: The University Press; 1903.
3. Gittinger JW Jr. Early investigations of x-ray by two Harvard-educated physicians revealed the technology's benefits—and dangers. Harvard Medical Alumni Bulletin. Spring 2008. [Cited 26 September 2014.] Available from: http://archive.org/stream/harvardmedicala81harv/harvardmedicala81harv_djvu.txt
4. Preston DL, Ron E, Tokuoka S, Funamoto S, Nishi N, Soda M, et al. Solid cancer incidence in atomic bomb survivors: 1958–1998. *Radiat Res* 2007; **168**: 1–64.
5. Brenner DJ, Doll R, Goodhead DT, Hall EJ, Land CE, Little JB, et al. Cancer risks attributable to low doses of ionizing radiation: assessing what we really know. *Proc Natl Acad Sci U S A* 2003; **100**: 13761–6.
6. Upton AC; National Coluncil on Radiation Protection and Measurements Scientific Committee 1-6. The state of the art in the 1990's: NCRP report no. 136 on the scientific bases for linearity in the dose–response relationship for ionizing radiation. *Health Phys* 2003; **85**: 15–22.
7. Brenner DJ, Hall EJ. Computed tomography–an increasing source of radiation exposure. *N Engl J Med* 2007; **357**: 2277–84.
8. Pearce MS, Salotti JA, Little MP, McHugh K, Lee C, Kim KP, et al. Radiation exposure from CT scans in childhood and subsequent risk of leukaemia and brain tumours: a retrospective cohort study. *Lancet* 2012; **380**: 499–505. doi: 10.1016/S0140-6736(12)60815-0
9. Mathews JD, Forsythe AV, Brady Z, Butler MW, Goergen SK, Byrnes GB, et al. Cancer risk in 680,000 people exposed to computed tomography scans in childhood or adolescence: data linkage study of 11 million Australians. *BMJ* 2013; **346**: f2360. doi: 10.1136/bmj.f2360
10. Ludlow JB. A manufacturer's role in reducing the dose of cone beam computed tomography examinations: effect of beam filtration. *Dentomaxillofac Radiol* 2011; **40**: 115–22. doi: 10.1259/dmfr/31708191
11. Bogdanich WMJ, Craven McGinty J. Radiation worries for children in dentists' chairs. The New York Times. 22 November 2010, Sect. A.
12. 1990 Recommendations of the International Commission on Radiological Protection. *Ann ICRP* 1991; **21**: 1–201.
13. The 2007 Recommendations of the International Commission on Radiological Protection. ICRP publication 103. *Ann ICRP* 2007; **37**: 1–332.
14. Ludlow JB, Davies-Ludlow LE, White SC. Patient risk related to common dental radiographic examinations: the impact of 2007 International Commission on Radiological Protection recommendations regarding dose calculation. *J Am Dent Assoc* 2008; **139**: 1237–43.
15. Ludlow JB, Ivanovic M. Comparative dosimetry of dental CBCT devices and 64-slice CT for oral and maxillofacial radiology. *Oral Surg Oral Med Oral Pathol Oral Radiol Endod* 2008; **106**: 106–14. doi: 10.1016/j.tripleo.2008.03.018
16. Vassileva J, Stoyanov D. Quality control and patient dosimetry in dental cone beam CT. *Radiat Prot Dosimetry* 2010; **139**: 310–12. doi: 10.1093/rpd/ncq011
17. Ludlow JB, Davies-Ludlow LE, Brooks SL. Dosimetry of two extraoral direct digital imaging devices: NewTom cone beam CT and Orthophos Plus DS panoramic unit. *Dentomaxillofac Radiol* 2003; **32**: 229–34.
18. Ludlow JB. Dose and risk in dental diagnostic imaging: with emphasis on dosimetry of CBCT. *Korean J Oral Maxillofac Radiol* 2009; **39**: 175–84.
19. Qu XM, Li G, Ludlow JB, Zhang ZY, Ma XC. Effective radiation dose of ProMax 3D cone-beam computerized tomography scanner with different dental protocols. *Oral Surg Oral Med Oral Pathol Oral Radiol Endod* 2010; **110**: 770–6. doi: 10.1016/j.tripleo.2010.06.013
20. Zhang G, Marshall N, Bogaerts R, Jacobs R, Bosmans H. Monte Carlo modeling for dose assessment in cone beam CT for oral and maxillofacial applications. *Med Phys* 2013; **40**: 072103. doi: 10.1118/1.4810967
21. Morant JJ, Salvado M, Hernandez-Giron I, Casanovas R, Ortega R, Calzado A. Dosimetry of a cone beam CT device for oral and maxillofacial radiology using Monte Carlo techniques and ICRP adult reference computational phantoms. *Dentomaxillofac Radiol* 2013; **42**: 92555893. doi: 10.1259/dmfr/92555893
22. Ludlow JB, Walker C. Assessment of phantom dosimetry and image quality of i-CAT FLX cone-beam computed tomography. *Am J Orthod Dentofacial Orthop* 2013; **144**: 802–17. doi: 10.1016/j.ajodo.2013.07.013
23. Martin CJ. Effective dose: how should it be applied to medical exposures? *Br J Radiol* 2007; **80**: 639–47.
24. Brenner D, Elliston C, Hall E, Berdon W. Estimated risks of radiation-induced fatal cancer from pediatric CT. *AJR Am J Roentgenol* 2001; **176**: 289–96.
25. Smith-Bindman R, Lipson J, Marcus R, Kim KP, Mahesh M, Gould R, et al. Radiation dose associated with common computed tomography examinations and the associated lifetime attributable risk of cancer. *Arch Intern Med* 2009; **169**: 2078–86. doi: 10.1001/archinternmed.2009.427
26. Richards AG, Barbor GL, Bader JD, Hale JD. Samarium filters for dental radiography. *Oral Surg Oral Med Oral Pathol* 1970; **29**: 704–15.
27. Underhill TE, Chilvarquer I, Kimura K, Langlais RP, McDavid WD, Preece JW, et al. Radiobiologic risk estimation from dental radiology: Part I. Absorbed doses to critical organs. *Oral Surg Oral Med Oral Pathol* 1988; **66**: 111–20.
28. Cristy M. Active bone marrow distribution as a function of age in humans. *Phys Med Biol* 1981; **26**: 389–400.
29. Physical aspects of irradiation. Washington DC: US Government Printing Office; 1964.
30. Pauwels R, Beinsberger J, Collaert B, Theodorakou C, Rogers J, Walker A, et al. Effective dose range for dental cone beam computed tomography scanners. *Eur J Radiol* 2012; **81**: 267–71. doi: 10.1016/j.ejrad.2010.11.028
31. Rottke D, Patzelt S, Poxleitner P, Schulze D. Effective dose span of ten different cone beam CT devices. *Dentomaxillofac Radiol* 2013; **42**: 20120417. doi: 10.1259/dmfr.20120417
32. Schilling R, Geibel MA. Assessment of the effective doses from two dental cone beam CT devices. *Dentomaxillofac Radiol* 2013; **42**: 20120273. doi: 10.1259/dmfr.20120273
33. Grunheid T, Kolbeck Schieck JR, Pliska BT, Ahmad M, Larson BE. Dosimetry of a cone-beam computed tomography machine compared with a digital x-ray machine in orthodontic imaging. *Am J Orthod Dentofacial Orthop* 2012; **141**: 436–43. doi: 10.1016/j.ajodo.2011.10.024
34. Davies J, Johnson B, Drage N. Effective doses from cone beam CT investigation of the jaws. *Dentomaxillofac Radiol* 2012; **41**: 30–6. doi: 10.1259/dmfr/30177908
35. Roberts JA, Drage NA, Davies J, Thomas DW. Effective dose from cone beam CT examinations in dentistry. *Br J Radiol* 2009; **82**: 35–40. doi: 10.1259/bjr/31419627
36. Kim DS, Rashsuren O, Kim EK. Conversion coefficients for the estimation of effective dose in cone-beam CT. *Imaging Sci Dent* 2014; **44**: 21–9. doi: 10.5624/isd.2014.44.1.21
37. Librizzi ZT, Tadinada AS, Valiyaparambil JV, Lurie AG, Mallya SM. Cone-beam computed tomography to detect erosions of the temporomandibular joint: Effect of field of view and voxel size on diagnostic efficacy and effective dose. *Am J Orthod Dentofacial Orthop* 2011; **140**: e25–30. doi: 10.1016/j.ajodo.2011.03.012
38. Jadu F, Yaffe MJ, Lam EW. A comparative study of the effective radiation doses from cone beam computed tomography and plain radiography for sialography. *Dentomaxillofac Radiol* 2010; **39**: 257–63. doi: 10.1259/dmfr/62878962

39. Qu XM, Li G, Sanderink GC, Zhang ZY, Ma XC. Dose reduction of cone beam CT scanning for the entire oral and maxillofacial regions with thyroid collars. *Dentomaxillofac Radiol* 2012; **41**: 373–8. doi: 10.1259/dmfr/30200901
40. Qu X, Li G, Zhang Z, Ma X. Thyroid shields for radiation dose reduction during cone beam computed tomography scanning for different oral and maxillofacial regions. *Eur J Radiol* 2012; **81**: e376–80. doi: 10.1016/j.ejrad.2011.11.048
41. Theodorakou C, Walker A, Horner K, Pauwels R, Bogaerts R, Jacobs R; SEDENTEXCT Project Consortium. Estimation of paediatric organ and effective doses from dental cone beam CT using anthropomorphic phantoms. *Br J Radiol* 2012; **85**: 153–60. doi: 10.1259/bjr/19389412
42. Lukat TD, Wong JC, Lam EW. Small field of view cone beam CT temporomandibular joint imaging dosimetry. *Dentomaxillofac Radiol* 2013; **42**: 20130082. doi: 10.1259/dmfr.20130082
43. Al-Okshi A, Nilsson M, Petersson A, Wiese M, Lindh C. Using GafChromic film to estimate the effective dose from dental cone beam CT and panoramic radiography. *Dentomaxillofac Radiol* 2013; **42**: 20120343. doi: 10.1259/dmfr.20120343
44. American Dental Association Council on Scientific Affairs, US Department of Health and Human Services Public Health Service, Food and Drug Administration. Dental radiographic examinations: recommendations for patient selection and limiting radiation exposure. American Dental Association; 2012. [Cited 26 September 2014.] Available from: www.fda.gov/Radiation-Emitting Products/Radiation Emitting Products and Procedures/MedicalImaging/Medical X-Rays/ucm116504.htm
45. National Council for Radiation Protection and Measurements. *NCRP report no. 145-radiation protection in dentistry*. Bethesda, MD: National Council on Radiation Protection and Measurement; 2003.
46. Okano T, Harata Y, Sugihara Y, Sakaino R, Tsuchida R, Iwai K, et al. Absorbed and effective doses from cone beam volumetric imaging for implant planning. *Dentomaxillofac Radiol* 2009; **38**: 79–85. doi: 10.1259/dmfr/14769929
47. Palomo JM, Rao PS, Hans MG. Influence of CBCT exposure conditions on radiation dose. *Oral Surg Oral Med Oral Pathol Oral Radiol* 2008; **105**: 773–82. doi: 10.1016/j.tripleo.2007.12.019
48. Loubele M, Bogaerts R, Van Dijck E, Pauwels R, Vanheusden S, Suetens P, et al. Comparison between effective radiation dose of CBCT and MSCT scanners for dentomaxillofacial applications. *Eur J Radiol* 2009; **71**: 461–8. doi: 10.1016/j.ejrad.2008.06.002
49. Ludlow JB, Davies-Ludlow LE, Brooks SL, Howerton WB. Dosimetry of 3 CBCT devices for oral and maxillofacial radiology: CB Mercuray, NewTom 3G and i-CAT. *Dentomaxillofac Radiol* 2006; **35**: 219–26.
50. Suomalainen A, Kiljunen T, Kaser Y, Peltola J, Kortesniemi M. Dosimetry and image quality of four dental cone beam computed tomography scanners compared with multislice computed tomography scanners. *Dentomaxillofac Radiol* 2009; **38**: 367–78. doi: 10.1259/dmfr/15779208
51. Jeong DK, Lee SC, Huh KH, Yi WJ, Heo MS, Lee SS, et al. Comparison of effective dose for imaging of mandible between multi-detector CT and cone-beam CT. *Imaging Sci Dent* 2012; **42**: 65–70. doi: 10.5624/isd.2012.42.2.65
52. Loubele M, Jacobs R, Maes F, Schutyser F, Debaveye D, Bogaerts R, et al. Radiation dose vs. image quality for low-dose CT protocols of the head for maxillofacial surgery and oral implant planning. *Radiat Prot Dosimetry* 2005; **117**: 211–16.
53. Ludlow JB. Comment on "effective dose range for dental cone beam computed tomography scanners". *Eur J Radiol* 2012; **81**: 4219–20; author reply 21–24. doi: 10.1016/j.ejrad.2012.05.027
54. HPAWPoDCBC Equipment. *Guidance on the safe use of dental cone beam CT (computed tomography) equipment. Report No HPA-CRCE-010*. Chilton, UK: Health Protection Agency; 2010.
55. European Commission. Cone beam CT for dental and maxillofacial radiology (evidence-based guidelines). 2011. [Cited 26 September 2014.] Available from: http://ec.europa.eu/energy/nuclear/radiation_protection/doc/publication/172.pdf
56. NCRP. Achievements of the past 50 years and addressing the needs of the future 2014. Fiftieth annual meeting of the National Council on Radiation Protection and Measurements (NCRP). Available from: http://www.ncrponline.org/Annual_Mtgs/2014_Ann_Mtg/PROGRAM_2-10.pdf